Sustainable Energy & Fuels

Enhanced photocatalytic hydrogen generation using carbazole-based sensitizers

Journal:	*Sustainable Energy & Fuels*
Manuscript ID	SE-COM-02-2017-000075
Article Type:	Communication
Date Submitted by the Author:	05-Feb-2017
Complete List of Authors:	Manfredi, Norberto; University of Milano-Bicocca, material science Monai, Matteo; University of Trieste, Montini, Tiziano; University of Trieste, Salamone, Matteo; University of Milano-Bicocca, Ruffo, Riccardo; University of Milano-Bicocca, Material Science Fornasiero, P; Univ. degli Studi di Trieste, Dipartimento di Scienze Chimiche Abbotto, Alessandro; University of Milano-Bicocca,

Journal Name

COMMUNICATION

Enhanced photocatalytic hydrogen generation using carbazole-based sensitizers

Received 00th January 20xx,
Accepted 00th January 20xx

DOI: 10.1039/x0xx00000x

www.rsc.org/

N. Manfredi,*[a] M. Monai,[b] T. Montini,[b] M. Salamone,[a] R. Ruffo,[a] P. Fornasiero,*[,b] and A. Abbotto*[,a]

ABSTRACT: Phenothiazine-, phenoxazine- and carbazole-based dyes have been synthesized and used as photosensitizers in Pt/TiO_2 films for photocatalytic hydrogen generation. Compared to commonly used phenothiazine dyes, planar and sulphur-free carbazole derivatives showed different molecular and supramolecular features which in turn yielded greatly enhanced (one order of magnitude) H_2 production performances.

The growing needs of present and future society concerning energy and sources for industrial chemical intermediates involve the research for sustainable technologies for production of fuels and chemicals.[1, 2] In this scenario, hydrogen, required for many industrial chemical processes and one of the possible energy vectors of the future, can be generated from renewable and cheap sources. The challenging photocatalytic water splitting [3-5] suffers of poor efficiency.[6] Ideally, this limitation can be partially overcome by enhancing the visible absorption.[7] In this respect, many approaches have been rather extensively exploited, ranging from homogeneous catalysis [8-10] to new generation semiconductor oxides [11] and composite nanomaterials.[12-14] Dye-sensitized photocatalysis is an alternatively and less investigated strategy to increase visible light absorption [15-20] The photocatalytic scheme implies the use of a tandem system with two components: a redox storing catalysts (such as the benchmark Pt/TiO_2) and a sensitizer able of absorbing a broad part of solar spectrum and of transferring electron to the catalysts. The photosensitizer must also be stable in the working condition under continuous irradiation over long periods of time. Thus, a rational design of the molecular structure of the dye must be developed to improve the stability and performances of sensitized photocatalysts. Various studies on dye-sensitized hydrogen generation involves the use of more traditional organometallic dyes.[21] Only recently, the focus is moving to metal-free sensitizers, which have the advantages of being cheaper, free of rare and toxic metals and endowed with a greater variety of structural and optical properties.[15, 18, 22-26]

We have recently reported a series of branched donor-(π-acceptor)$_2$ phenothiazine-based sensitizers (**PTZ**) functionalized with an alkyl terminal and containing different thiophene-based spacer,[27] showing lower activity but improved stability with respect to the reference system without the thiophene spacer. This fact has been related with electronic and steric effect of the thiophene spacer, favouring charge separation after light excitation of the donor group (phenothiazine) but probably inducing sulphur poisoning phenomena on surface of the Pt nanoparticles.

In this work, the effect of molecular design of the dye on the photocatalytic hydrogen generation is investigated by sequentially removing sulphur-based units from the chemical structure of the dye. In particular, new sensitizers have been prepared by replacing the **PTZ** donor core with a sulphur-free electron-rich heteroaromatic ring and replacing the thiophene spacers with a sulphur-free heteroaromatic analogue. The introduction of the carbazole (**CBZ**) moiety in the molecular structure afforded a strong enhancement of the efficiency of photocatalytic H_2 production compared to both **PTZ** and phenoxazine (**POZ**) based dyes, using Pt/TiO_2 as benchmark redox storing catalyst. The amount of produced hydrogen and turnover numbers (TON) are top-ranked amongst studies on dye-sensitized photocatalytic hydrogen production.

The **CBZ** building block has been selected as an ideal sulphur-free alternative to **PTZ**, being a strong electron-rich heteroaromatic ring thanks to the presence of the central five-membered ring containing a pyrrole-like nitrogen atom.[28] Despite **CBZ** is highly investigated for its applications in in materials science,[29-32] and in dye-sensitized solar cell (DSSCs),[33-36] only very few studies on photocatalysis have been reported.[37-39] Remarkably, whereas **PTZ** are associated to a typical butterfly structure,[40, 41] **CBZ** is planar, suggesting a

[a] *Department of Materials Science and Solar Energy Research Center MIB-SOLAR, University of Milano-Bicocca, and INSTM Milano-Bicocca Research Unit, Via Cozzi 55, I-20125, Milano, Italy.*
[b] *Department of Chemical and Pharmaceutical Sciences, INSTM Trieste Research Unit and ICCOM-CNR Trieste Research Unit, University of Trieste, via L. Giorgieri 1, I-34127, Trieste, Italy.*

Electronic Supplementary Information (ESI) available: synthetic scheme and procedures, optical end electrochemical parameters, CV, DPV, overall activity results, ^{1}H-NMR and ^{13}C-NMR. See DOI: 10.1039/x0xx00000x

strong effect of the charge generation and transport properties on catalytic efficiency of the tandem system. In order to separate the effects of the replacement of the S atom and of the change in the spatial arrangement, we have also investigated **POZ** donor groups. Within the scope of this work, **POZ** has the advantage of maintaining the butterfly structure as in **PTZ**, permitting to better elucidate the role of the **CBZ** unit.

To investigate the role of S in the spacer unit, we have designed new dyes by replacing the thiophene (**Th**) π-bridge with its sulphur-free five-membered analogue furan ring (**Fu**), which shares with thiophene many electronic and structural properties with the exception of the nature of the ring heteroatom.[28] The structures of new dyes are summarized in Fig 1, being **PTZ-Th** the reference system.[27]

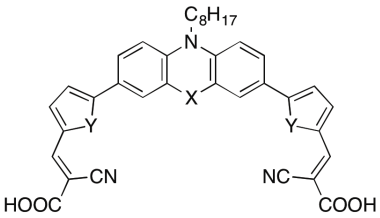

PTZ-Th: X = S, Y = S
PTZ-Fu: X = S, Y = O
POZ-Th: X = O, Y = S
POZ-Fu: X = O, Y = O
CBZ-Th: X = none, Y = S
CBZ-Fu: X = none, Y = O

Fig 1 Dyes investigated in this work.

PTZ-Th has been synthesized according to the literature.[27] The same synthetic scheme (Scheme S1) has been adopted as a simple and easily extendible procedure for synthesis of the new dyes. The development of a general procedure (See ESI) is not only relevant for industrial scale-up but also to easily access an extended library of dyes. Although the synthesis of **CBZ-Th** and a molecule similar to **CBZ-Fu** (bearing a different *N*-alkyl functionalization) have been previously reported in the literature,[35, 42] the **CBZ**-based sensitizers were synthesized by the aforementioned general approach using 3,6-dibromocarbazole as a starting reagent while **POZ** derivatives were synthesized from 10-octyl-10H-phenooxazine-3,7-dibromo.[43] **Fu** and **Th** derivatives have been prepared connecting the donor and the spacer units by Suzuki cross-coupling reaction using the commercially available 2-furan-aldehyde-5-boronic acid and 2-thiophene-aldehyde-5-boronic acid, respectively.

The absorption spectra of the dyes (10^{-5} M in DMSO) are shown in Fig 2 and the detailed main optical and energetic parameters (HOMO-LUMO energies) are listed in Table S1. In general, the three families of **PTZ**, **POZ** and **CBZ** dyes exhibited the typical 2 bands, related to π-π* absorption in the 300 – 450 nm range and to the intramolecular charge transfer (ICT) transition in the 400-600nm range. [35, 44] The π-π* band shows a progressive red-shift in the order **POZ**-**PTZ**-**CBZ** as a result of increased electron delocalization in the core. On the other hand, the ICT transition is subjected to a progressive blue-shift. As a result, π-π* and ICT transitions significantly overlap for the **CBZ** derivatives. The absorption maxima are centered around *ca.* 470 nm for **PTZ**, ca. 410 nm for **CBZ** and ca. 530 nm for the **POZ** dyes. Importantly, the maximum molar absorptivity is higher for the **CBZ** derivatives, whereas marginal differences (less than 10%) are recorded between **PTZ** and **POZ** analogs. Finally, the introduction of the **Fu** spacer in place of **Th** did not significantly affect the absorption properties.

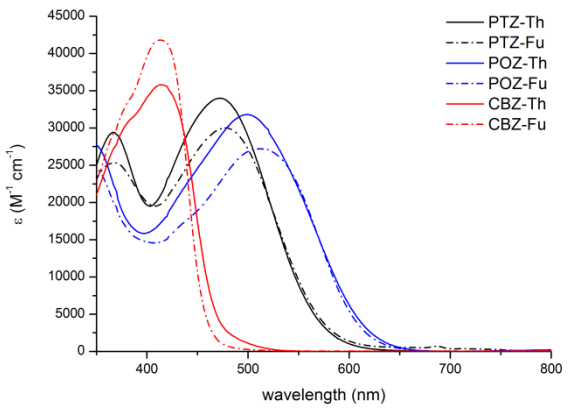

Fig 2 Absorption spectra of the **PTZs**, **CBZs** and **POZs** dyes recorded in DMSO solution.

The electrochemical properties have been investigated for all the dyes and the main optical and electrochemical parameters are summarized in Table S1 (see ESI). Cyclic voltammetry (CV) profiles (Figure S1, ESI) showed a quasi-reversible behavior for the oxidation process in all the investigated dyes, whereas reduction was irreversible. Differential Pulsed Voltammetry (DPV) results (Figure S2, ESI) was used to determine the HOMO energy levels from the current peak.[45] The LUMO levels have been derived from electrochemical HOMO values and optical bandgaps, measured by means of Tauc plots.[46] Levels are pictorially shown in Figure S3 (see ESI) and reported in Table S1 (see ESI). Even though the HOMO energy levels are quite similar for most of the dyes (~ -5.60 eV), the different bandgaps significantly affect their LUMO energies and, accordingly, the electron injection capabilities to the Pt/TiO_2 system. In particular, the LUMO energy of the **POZ** dyes, as well as that of **PTZ-Fu**, are very close to the conduction band (CB) of TiO_2 (-4.0eV).[47]

The sensitized Pt/TiO_2 photocatalysts were tested for H_2 production under Visible light irradiation (λ > 420 nm) from a triethanolamine (TEOA)/HCl aqueous buffer solution at pH = 7.0. The experiments have been performed adopting the same conditions previously optimized for **PTZ**-based photocatalysts.[48, 49] No H_2 production was observed using the bare Pt/TiO_2 under the same experimental conditions. Measured H_2 production rates and H_2 productivity vs irradiation time are presented in Figs. S4 and S5 (see ESI), respectively. Turnover numbers (TON) and Light-to-Fuel Efficiency (LFE_{20}) calculated after 20 h of irradiation are presented in Fig 3 (obtained values are listed in Table S2, ESI).

All of the investigated catalysts showed remarkable stability over a reasonable irradiation time of 20 h (Figure S4, ESI). **CBZ**-sensitized photocatalysts showed by far the highest H_2 productivities, TON and LFE values. Namely, performances were at least one order of magnitude higher than those referred to the benchmark **PTZ-Th** dye. Amongst **CBZ** based

dyes, the photocatalytic activity of **CBZ-Th** was considerably higher than that of **CBZ-Fu**. The same relative trend was recorded for the **PTZ** family. Both **POZs**-sensitized photocatalysts demonstrated very small activity in H_2 production.

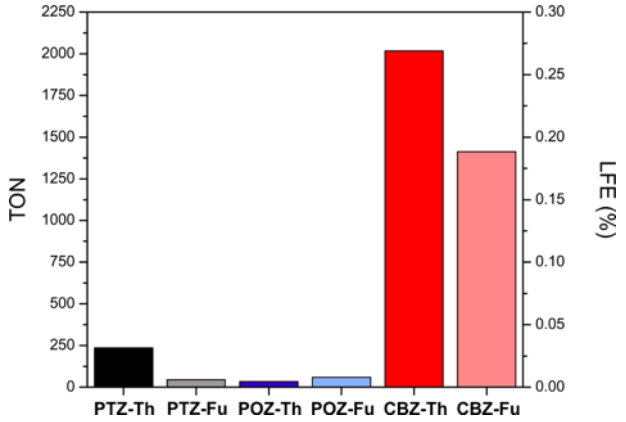

Fig 3 Turnover number (TON) and Light-to-Fuel Efficiencies (LFE) calculated from H_2 production using TEOA/HCl solution at pH = 7.0 under irradiation with visible light (λ > 420 nm) over Pt/TiO_2 materials sensitized with **PTZs**, **POZs** and **CBZs** dyes.

Such an enhancement can be rationalized in terms of the planar spatial arrangement of the **CBZ** donor group, which in turns positively affects the charge generation, transport properties, and catalytic efficiency of the tandem system. **CBZ-Th** showed a red-shifted visible light absorption (up to 600 nm) when adsorbed on the surface of TiO_2, as well as a broadening of the absorption spectrum (Fig S6, ESI) after long staining time, according to previous observations for analogous derivatives.[35] These data might suggest the occurrence of some kind of self-organization on the surface of the semiconductor induced by the planar structure of the **CBZ** donor core. A similar behaviour has not previously reported for corresponding similar phenothiazine and phenoxazine derivatives.[50] Such different arrangement of photosensitizer molecules on the surface of the semiconductor film may provide one of the main reasons for the different observed spectroscopic and photocatalytic properties of the **CBZ** derivatives. To better investigate this phenomenon, the absorption spectrum of **CBZ-Th** was recorded in presence of chenodeoxycholic acid (CDCA), a widely used co-adsorbing and disaggregating agent (Fig S7, ESI).[51] The results revealed that the presence of CDCA, even in relatively high quantity, does not affect the optical properties of the adsorbed dyes. Accordingly, the photocatalytic activity in presence of CDCA gave similar results as that without the co-adsorbent (Fig S8, ESI). This is a clear suggestion that the role of supramolecular aggregates, if present, is not predominant and thus is not likely the main cause of the recorded enhanced photocatalytic performance.

In addition to the above discussed dye-sensitization mechanism, the improved photocatalytic can originate from a ligand-to-metal charge transfer (LMCT) phenomenon.[52, 53] The LMCT mechanism is observed when charge transfer takes place after formation of complexes between TiO_2 and the surface adsorbates. LMCT species absorb in the Visible range whereas neither of TiO_2 and the organic adsorbates typically absorb Visible light. Upon coupling with TiO_2, electron-rich organic compounds with linker groups (e.g., cathecol, carrying two ortho OH anchoring groups) exhibit a LMCT band in the visible region, as a result of the strong coupling between the molecular orbital (HOMO) of the adsorbate and the energy band of the semiconductor. In this case, the absorption of a photon allows the excitation of an electron directly from the ground state (HOMO level) of the adsorbate (ligand) to the semiconductor CB with mainly metal orbital characters, without involving the excited state of the adsorbate. This mechanism has been scantly investigated in DSSCs in presence of simple cathecol-based molecule resulting in a modest increase of the power conversion efficiency.[54, 55] Since the peculiar feature of the LMCT is the formation of a band around 600 nm, in highly π-conjugated molecules it is more difficult to distinguish the presence of the LMCT band in presence of the visible ICT band of common dyes employed in TiO_2 sensitization. In the case of LMCT, the nature of the sensitizers can drastically affect the back electron transfer from TiO_2 to the oxidized sensitizer. Furthermore, it was showed that a large portion (>75%) of charge recombination occurs within a few picoseconds in the LMCT sensitization.[54] Based on these considerations, it is difficult to unequivocally prove the presence of the LMCT mechanism in the present **CBZ** dyes, though the presence of an absorption tail in the 600 nm region may suggest that. We argue that the combined effects of different surface molecular arrangement and LMCT are responsible for the increased efficiency of **CBZ** dyes, as a result of a more efficient light harvesting. To investigate the presence of a similar mechanism in the **PTZ** and **POZ** dyes, H_2 productivity has been checked using a cut-off filter at 515 nm (Fig S9, ESI). After activation of the photocatalysts for 8 h under the usual conditions, **CBZ-Th** still shows an appreciable photocatalytic activity whereas H_2 production completely disappeared for **PTZ-Th**, despite its intense light absorption up to 600 nm. This fact suggests that in the latter dye the longer wavelength band is very less efficient in promoting the photocatalytic H_2 production. Taking this into account, the low activity observed under irradiation with λ > 420 nm using **PTZ** and **POZ** dyes as sensitizers (Fig 3) could be related to the lower efficiency of the π-π* transition in the photocatalytic cycle.

In conclusion, a rational design of the sensitizers was shown to be the key to obtain greatly enhanced performances in H_2 photogeneration under visible light irradiation. The presence of heteroatoms in the donor group and spacer moieties of the investigated sensitizers dramatically affect the photocatalytic H_2 production in the visible range over Pt/TiO_2. In particular, the replacement of butterfly-like phenothiazine derivatives with planar, sulphur-free carbazole dyes provided different molecular and supramolecular properties. These features in turn afforded greatly enhanced (one order of magnitude) dye-sensitized hydrogen generation performances, amongst the

best ever reported in the literature for photocatalytic systems based on organic photosensitizers.[15]

Notes and references

University of Milano-Bicocca, University of Trieste (through project FRA 2015), Beneficientia Stiftung, ICCOM-CNR and INSTM are kindly acknowledged for financial support.

1. N. Armaroli and V. Balzani, in *Energy for a Sustainable World*, Wiley-VCH Verlag GmbH & Co. KGaA, 2010, DOI: 10.1002/9783527633593.fmatter.
2. G. A. Ozin, *Energy Environ. Sci.*, 2015, **8**, 1682-1684.
3. A. Fujishima and K. Honda, *Nature*, 1972, **238**, 37-38.
4. K. Kalyanasundaram and M. Graetzel, *Curr. Opin. Biotechnol.*, 2010, **21**, 298-310.
5. Y. Tachibana, L. Vayssieres and J. R. Durrant, *Nat Photon*, 2012, **6**, 511-518.
6. N. Armaroli and V. Balzani, *ChemSusChem*, 2011, **4**, 21-36.
7. V. Balzani, A. Credi and M. Venturi, *ChemSusChem*, 2008, **1**, 26-58.
8. T. M. McCormick, B. D. Calitree, A. Orchard, N. D. Kraut, F. V. Bright, M. R. Detty and R. Eisenberg, *J. Am. Chem. Soc.*, 2010, **132**, 15480-15483.
9. P. Du, K. Knowles and R. Eisenberg, *J. Am. Chem. Soc.*, 2008, **130**, 12576-12577.
10. S. Losse, J. G. Vos and S. Rau, *Coord. Chem. Rev.*, 2010, **254**, 2492-2504.
11. X. Chen, S. Shen, L. Guo and S. S. Mao, *Chem Rev*, 2010, **110**, 6503-6570.
12. W. Fan, Q. Zhang and Y. Wang, *Phys. Chem. Chem. Phys.*, 2013, **15**, 2632-2649.
13. A. Beltram, M. Melchionna, T. Montini, L. Nasi, P. Fornasiero and M. Prato, *Green Chem.*, 2017, DOI: 10.1039/c6gc01979j.
14. H. Wang, L. Zhang, Z. Chen, J. Hu, S. Li, Z. Wang, J. Liu and X. Wang, *Chem. Soc. Rev.*, 2014, **43**, 5234-5244.
15. B. Cecconi, N. Manfredi, T. Montini, P. Fornasiero and A. Abbotto, *Eur. J. Org. Chem.*, 2016, **2016**, 5194-5215.
16. X. H. Zhang, T. Y. Peng and S. S. Song, *J. Mater. Chem. A*, 2016, **4**, 2365-2402.
17. X. Zhang, L. Yu, C. Zhuang, T. Peng, R. Li and X. Li, *Acs Catal*, 2014, **4**, 162-170.
18. M. Watanabe, H. Hagiwara, A. Iribe, Y. Ogata, K. Shiomi, A. Staykov, S. Ida, K. Tanaka and T. Ishihara, *J. Mater. Chem. A*, 2014, **2**, 12952-12961.
19. F. Li, K. Fan, B. Xu, E. Gabrielsson, Q. Daniel, L. Li and L. Sun, *J. Am. Chem. Soc.*, 2015, **137**, 9153-9159.
20. K. A. Click, D. R. Beauchamp, Z. Huang, W. Chen and Y. Wu, *J. Am. Chem. Soc.*, 2016, **138**, 1174-1179.
21. Z. Yu, F. Li and L. Sun, *Energy Environ. Sci.*, 2015, **8**, 760-775.
22. X. Li, S. C. Cui, D. Wang, Y. Zhou, H. Zhou, Y. Hu, J. G. Liu, Y. T. Long, W. J. Wu, J. L. Hua and H. Tian, *Chemsuschem*, 2014, **7**, 2879-2888.
23. L. Yu, X. Zhang, C. Zhuang, L. Lin, R. Li and T. Peng, *Phys. Chem. Chem. Phys.*, 2014, **16**, 4106-4114.
24. N. Queyriaux, N. Kaeffer, A. Morozan, M. Chavarot-Kerlidou and V. Artero, *J. Photochem. Photobiol. C: Photochem. Rev.*, 2015, **25**, 90-105.
25. F. Ronconi, Z. Syrgiannis, A. Bonasera, M. Prato, R. Argazzi, S. Caramori, V. Cristino and C. A. Bignozzi, *J. Am. Chem. Soc.*, 2015, **137**, 4630-4633.
26. N. Kaeffer, J. Massin, C. Lebrun, O. Renault, M. Chavarot-Kerlidou and V. Artero, *J. Am. Chem. Soc.*, 2016, **138**, 12308-12311.
27. B. Cecconi, N. Manfredi, R. Ruffo, T. Montini, I. Romero-Ocana, P. Fornasiero and A. Abbotto, *ChemSusChem*, 2015, **8**, 4216-4228.
28. A. R. Katritzky and C. W. Rees, *Comprehensive Heterocyclic Chemistry*, Pergamon, Oxford, 1984.
29. A. W. Schmidt, K. R. Reddy and H.-J. Knölker, *Chem. Rev.*, 2012, **112**, 3193-3328.
30. G. Sathiyan, E. K. T. Sivakumar, R. Ganesamoorthy, R. Thangamuthu and P. Sakthivel, *Tetrahedron Lett.*, 2016, **57**, 243-252.
31. J. Li and A. C. Grimsdale, *Chem. Soc. Rev.*, 2010, **39**, 2399-2410.
32. H. Jiang, *Asian J Org Chem*, 2014, **3**, 102-112.
33. N. Manfredi, B. Cecconi and A. Abbotto, *Eur. J. Org. Chem.*, 2014, DOI: 10.1002/ejoc.201402422, 7069-7086.
34. C. Chen, J.-Y. Liao, Z. Chi, B. Xu, X. Zhang, D.-B. Kuang, Y. Zhang, S. Liu and J. Xu, *J. Mater. Chem.*, 2012, **22**, 8994-9005.
35. K. S. V. Gupta, T. Suresh, S. P. Singh, A. Islam, L. Han and M. Chandrasekharam, *Org. Electron.*, 2014, **15**, 266-275.
36. S. Pramjit, U. Eiamprasert, P. Surawatanawong, P. Lertturongchai and S. Kiatisevi, *J. Photochem. Photobiol. A: Chem.*, 2015, **296**, 1-10.
37. R. Abe, K. Shinmei, N. Koumura, K. Hara and B. Ohtani, *J. Am. Chem. Soc.*, 2013, **135**, 16872-16884.
38. R. S. Sprick, B. Bonillo, R. Clowes, P. Guiglion, N. J. Brownbill, B. J. Slater, F. Blanc, M. A. Zwijnenburg, D. J. Adams and A. I. Cooper, *Angew. Chem. Int. Ed.*, 2016, **55**, 1792-1796.
39. C. Su, R. Tandiana, B. Tian, A. Sengupta, W. Tang, J. Su and K. P. Loh, *Acs Catal*, 2016, **6**, 3594-3599.
40. J. McDowell, *Acta Crystallogr. Sect. B: Struct. Sci.*, 1976, **32**, 5-10.
41. S. S. Park, Y. S. Won, Y. C. Choi and J. H. Kim, *Energy & Fuels*, 2009, **23**, 3732-3736.
42. R. Grisorio, L. De Marco, G. Allegretta, R. Giannuzzi, G. P. Suranna, M. Manca, P. Mastrorilli and G. Gigli, *Dyes Pigm.*, 2013, **98**, 221-231.
43. J. Soloducho, J. Doskocz, A. Nowakowska, J. Cabaj, M. Lapkowski and S. Golba, *Pol. J. Chem.*, 2007, **81**, 2001 - 2012.
44. X. Liu, J. Long, G. Wang, Y. Pei, B. Zhao and S. Tan, *Dyes Pigm.*, 2015, **121**, 118-127.
45. K. Izutsu, in *Electrochemistry in Nonaqueous Solutions*, Wiley-VCH Verlag GmbH & Co. KGaA, 2009, DOI: 10.1002/9783527629152.fmatter.
46. J. Tauc, *Mater. Res. Bull.*, 1968, **3**, 37-46.
47. *Dye Sensitized Solar Cells*, CRC Press, Boca Raton, FL, USA, K.Kalyanasundaram edn., 2010.
48. H. Kisch and D. Bahnemann, *J. Phys. Chem. Lett.*, 2015, **6**, 1907-1910.
49. N. Manfredi, B. Cecconi, V. Calabrese, A. Minotti, F. Peri, R. Ruffo, M. Monai, I. Romero-Ocana, T. Montini, P. Fornasiero and A. Abbotto, *Chem. Commun.*, 2016, **52**, 6977-6980.

50. W.-I. Hung, Y.-Y. Liao, C.-Y. Hsu, H.-H. Chou, T.-H. Lee, W.-S. Kao and J. T. Lin, *Chem. Asian J.*, 2014, **9**, 357-366.
51. K.-M. Lee, C.-Y. Chen, S.-J. Wu, S.-C. Chen and C.-G. Wu, *Sol. Energy Mater. Sol. Cells*, 2013, **108**, 70-77.
52. H. Park, H.-i. Kim, G.-h. Moon and W. Choi, *Energy Environ. Sci.*, 2016, **9**, 411-433.
53. G. Zhang, G. Kim and W. Choi, *Energy Environ. Sci.*, 2014, **7**, 954-966.
54. Y. Ooyama, M. Kanda, K. Uenaka and J. Ohshita, *Chemphyschem*, 2015, **16**, 3049-3057.
55. E. L. Tae, S. H. Lee, J. K. Lee, S. S. Yoo, E. J. Kang and K. B. Yoon, *J. Phys. Chem. B*, 2005, **109**, 22513-22522.

Enhanced H_2 production in carbazole based dyes in dye-sensitized photocatalysis

N. Manfredi,[*,†] M. Monai, [‡] T. Montini,[‡] M. Salamone,[†] R. Ruffo,[†] P. Fornasiero,[*, ‡] and A. Abbotto[*,†]

Electronic Supplementary Material

General information

NMR spectra were recorded with a Bruker AMX-500 spectrometer operating at 500.13 MHz (^{1}H) and 125.77 MHz (^{13}C). Coupling constants are given in Hz. Absorption spectra were recorded with a V-570 Jasco spectrophotometer. Infrared spectra (IR) were recorded with an ATR-FTIR Perkin–Elmer Spectrum100 spectrometer. Flash chromatography was performed with Merck grade 9385 silica gel 230–400 mesh (60 Å). Reactions performed under inert atmosphere were done in oven-dried glassware and a nitrogen atmosphere was generated with Schlenk technique. Conversion was monitored by thin-layer chromatography by using UV light (254 and 365 nm) as a visualizing agent. All reagents were obtained from commercial suppliers at the highest purity grade and used without further purification. Anhydrous solvents were purchased from Sigma-Aldrich and used without further purification. Extracts were dried with Na_2SO_4 and filtered before removal of the solvent by evaporation. Compounds **1a-c, 2a** and **PTZ-Th** have been prepared according to literature.[1-3]

Scheme S1: General synthetic procedure for dyes **PTZs**, **POZs**, **CBZs**.

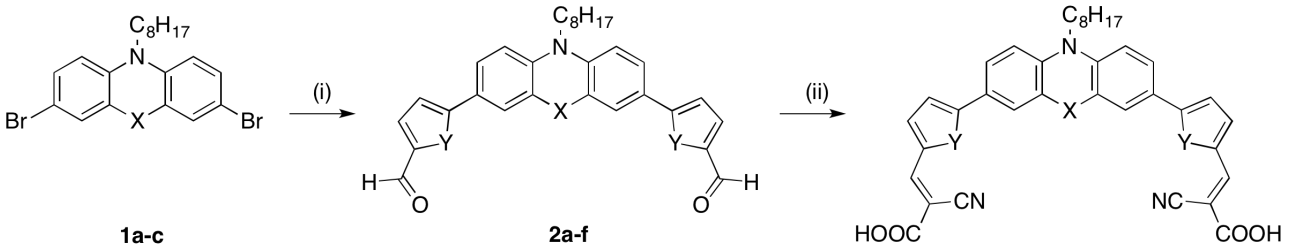

1a-c **2a-f**

a: X = S
b: X = O
c: X = none

a: X = S, Y = S
b: X = S, Y = O
c: X = O, Y = S
d: X = O, Y = O
e: X = none, Y = S
f: X = none, Y = O

PTZ-Th: X = S, Y = S
PTZ-Fu: X = S, Y = O
POZ-Th: X = O, Y = S
POZ-Fu: X = O, Y = O
CBZ-Th: X = none, Y = S
CBZ-Fu: X = none, Y = O

Reagents and conditions: (i) 5-Formyl-2-aryl-boronic acid, $Pd(dppf)Cl_2 \cdot CH_2Cl_2$ [dppf = 1,1′-bis(diphenylphosphino)ferrocene], K_2CO_3, DME/MeOH, microwave 100 °C, 90 min; (ii) cyanoacetic acid, piperidine, $CHCl_3$, reflux, 5 h.

Synthetic procedures

General Procedure for Suzuki-Miyaura Cross-Coupling: Product **1** (1 eq.) and $Pd(dppf)Cl_2 \cdot CH_2Cl_2$ (10 % eq.) were dissolved in dimethoxyethane (0.1 M) and stirred for 15 minutes under nitrogen atmosphere. Then boronic acid derivative (2.4 eq.) and K_2CO_3 (10 eq.) were added as suspension in methanol (0.1 M). The reaction was performed with microwave irradiation (100 °C, 200 watt, 90 minutes) and then quenched by pouring into a saturated solution of NH_4Cl (50 mL). Filtration on Celite and extractions with organic solvent allowed to isolate the crude product, then purified through column chromatography on silica gel.

General Procedure for Knoevenagel Condensation: Aldehyde precursor (1 eq.), cyanoacetic acid (10 eq.) and piperidine (10 eq. + catalytic) were dissolved in $CHCl_3$ (0.02 M) and warmed to reflux for 5 h. After having the solvent evaporated, a solution of HCl 1 M (~50 mL) was added and the mixture was left under magnetic stirring for 5 h at rt. The dark red solid that precipitated was filtered and washed with water (3x30 mL), PE (2x30 mL) and Et_2O (1x10 mL).

5,5'-(10-octyl-10*H*-phenothiazine-3,7-diyl)difuran-2-carbaldehyde (2b). Product **2b** was synthetized according to general procedure for Suzuki-Miyaura cross-coupling, using product **1a** (330 mg, 0.71 mmol), $Pd(dppf)Cl_2 \cdot CH_2Cl_2$ (57 mg, 0.071 mmol), (5-formylfuran-2-yl)boronic acid (240 mg, 1.7 mmol), K_2CO_3 (980 mg, 7.1 mmol), DME (3 mL) and methanol (3 mL). Extractions were performed with CH_2Cl_2 (3 x 50 mL) and a mixture of PE:AcOEt – 7:3 was used as eluent for purification. The desired product was isolated as a red solid (160 mg) with a 45% of yield. ^{1}H NMR (500 MHz, $CDCl_3$) δ 9.60 (s, 2H), 7.58 (dd, J = 8.5, 1.9 Hz, 2H), 7.52 (d, J = 1.9 Hz, 2H), 7.28 (d, J = 3.7 Hz, 2H), 6.86 (d, J = 8.6 Hz, 2H), 6.71 (d, J = 3.7 Hz, 2H), 3.86 (t, J = 7.2 Hz, 2H), 1.86 – 1.74 (m, 2H), 1.50 – 1.37 (m, 2H), 1.36 – 1.18 (m, 8H), 0.86 (t, J = 6.9 Hz, 3H). ^{13}C NMR (126 MHz, $CDCl_3$) δ.76, 158.67, 151.82, 145.39, 124.75, 124.59, 124.06, 123.78, 115.55, 106.77, 47.90, 31.65, 29.11, 29.08, 26.75, 26.71, 22.53, 13.98.

5,5'-(10-octyl-10*H*-phenooxazine-3,7-diyl)dithiophene-2-carbaldehyde (2c). Product **2c** was synthetized according to general procedure for Suzuki-Miyaura cross-coupling, using product **1b** (300 mg, 0.66 mmol), Pd(dppf)Cl_2·CH_2Cl_2 (54 mg, 0.066 mmol), (5-formylthiophen-2-yl)boronic acid (247 mg, 1.58 mmol), K_2CO_3 (910 mg, 6.6 mmol), DME (3 mL) and methanol (3 mL). Extractions were performed with AcOEt (3 x 50 mL) and a mixture of PE:AcOEt - 3:1 was used as eluent for purification. The desired product was isolated as a red-orange solid (50 mg) with a 15% of yield. ^{1}H-NMR ($CDCl_3$, 500 MHz): δ 9.84 (s, 2H), 7.68 (d, 2H, *J* = 4.0 Hz), 7.24 (d, 2H, *J* = 4.0 Hz), 7.14 (dd, 2H, *J* = 8.4, 2.0 Hz), 6.93 (d, 2H, *J* = 2.0 Hz), 6.49 (d, 2H, *J* = 8.4 Hz), 3.50 (t, 2H, *J* = 8.0 Hz), 1.67 (q, 2H, *J* = 8.0 Hz), 1.45-1.20 (m, 10H), 0.89 (t, 3H, *J* = 6.8 Hz). ^{13}C-NMR ($CDCl_3$, 126 MHz): δ 182.48, 153.48, 144.78, 141.26, 137.57, 133.51, 126.37, 122.76, 122.31, 113.06, 111.80, 44.24, 31.75, 29.68, 29.31, 29. 23, 26.86, 25.10, 22.60, 14.06.

5,5'-(10-octyl-10*H*-phenooxazine-3,7-diyl)furan-2-carbaldehyde (2d). Product **2d** was synthetized according to general procedure for Suzuki-Miyaura cross-coupling, using product **1** (300 mg, 0.66 mmol), Pd(dppf)Cl_2·CH_2Cl_2 (54 mg, 0.066 mmol), (5-formylfuran-2-yl)boronic acid (221 mg, 1.58 mmol), K_2CO_3 (910 mg, 6.6 mmol), DME (3 mL) and methanol (3 mL). Extractions were performed with AcOEt (3 x 50 mL) and a mixture of CH_2Cl_2/PE - 97:3 was used as eluent for purification. The desired product was isolated as a dark red solid (200 mg) with a 63% of yield. ^{1}H-NMR ($CDCl_3$, 500 MHz): δ 9.55 (s, 2H), 7.26 (d, 2H, *J* = 3.7 Hz), 7.24 (dd, 2H, *J* = 8.4, 2.0 H), 6.98 (d, 2H, *J* = 2.0 Hz), 6.62 (d, 2H, *J* = 3.7 Hz), 6.45 (d, 2H, *J* = 8.4 Hz), 3.45 (t, 2H, *J* = 7.8 Hz), 1.63 (q, 2H, *J* = 7.6 Hz), 1.45-1.20 (m, 10H), 0.89 (t, 3H, *J* = 6.7 Hz). ^{13}C-NMR ($CDCl_3$, 126 MHz): δ 176.64, 158.85, 151.51, 144.73, 133.66, 122.24, 121.46, 112.08, 111.63, 106.46, 44.21, 31.74, 29.28, 29.22, 26.81, 25.07, 22.60, 14.06.

5,5'-(9-Octyl-9H-carbazole-3,6-diyl)dithiophene-2-carbaldehyde (2e). Product **2e** was synthetized according to general procedure for Suzuki-Miyaura cross-coupling, using product **1c** (253 mg, 0.58 mmol), Pd(dppf)Cl_2·CH_2Cl_2 (48 mg, 0.059 mmol), (5-formylthiophen-2-yl)boronic acid (225 mg, 1.44 mmol), K_2CO_3 (790 mg, 5.75 mmol), DME (3 mL) and methanol (3 mL). Extractions were performed with AcOEt (3 x 50 mL) and a mixture of CH_2Cl_2/Et_2O - 95:5 was used as eluent for purification. The desired product was isolated as a red solid (210 mg) with a 72% of yield. ^{1}H NMR (500 MHz, $CDCl_3$): δ 9.89 (s, 2H), 8.40 (d, *J* = 1.7 Hz, 2H), 7.80 (dd, *J* = 8.6 Hz, 1.8 Hz, 2H), 7.77 (d, *J* = 4.0 Hz, 2H), 7.47 (d, *J* = 3.9 Hz, 2H), 7.43 (d, *J* = 8.6 Hz, 2H), 4.30 (t, *J* = 7.3 Hz, 2H), 1.88 (q, *J* = 7.3Hz, 2H), 1.41-1.19 (m, 10H), 0.87 (t, *J* = 6.8 Hz, 3H).

5,5'-(9-Octyl-9H-carbazole-3,6-diyl)difuran-2-carbaldehyde (2f). Product **2f** was synthetized according to general procedure for Suzuki-Miyaura cross-coupling, using product **1c** (253 mg, 0.58 mmol), Pd(dppf)Cl_2·CH_2Cl_2 (49 mg, 0.059 mmol), (5-formylfuran-2-yl)boronic acid (193 mg, 1.38 mmol), K_2CO_3 (788 mg, 5.71 mmol), DME (3 mL) and methanol (3 mL). Extractions were performed with CH_2Cl_2 (3 x 50 mL) and a mixture of CH_2Cl_2:AcOEt - 9:1 was used as eluent for purification. The desired product was isolated as a red solid (159 mg) with a 59% of yield. ^{1}H NMR (500 MHz, $CDCl_3$): δ 9.65 (s, 2H), 8.60 (d, *J* = 1.4 Hz, 2H), 7.94 (dd, *J* = 8.6 Hz, 1.7 Hz, 2H), 7.42 (d, *J* = 8.6 Hz, 2H), 7.37 (d, *J* = 3.8 Hz, 2H), 6.88 (d, *J* = 3.7 Hz, 2H), 4.28 (t, *J* = 7.3 Hz, 2H), 1.87 (q, *J* = 7.4 Hz, 2H), 1.42-1.18 (m, 10H), 0.86 (t, *J*= 7.0 Hz, 3H). ^{13}C-NMR ($CDCl_3$, 126 MHz): δ 176.76,160.76, 151.63, 141.57, 123.90, 123.14, 120.76, 118.11, 109.53, 106.39, 43.46, 31.73, 29.28, 29.12, 28.97, 27.23, 22.57, 14.04.

3,3'-(5,5'-(10-octyl-10*H*-phenothiazine-3,7-diyl)bis(furan-5,2-diyl))bis(2-cyanoacrylic acid) (PTZ-Fu). **PTZ-Fu** was synthetized according to general procedure for Knoevenagel condensation using product **2b** (160 mg, 0.32 mmol), cyanoacetic acid (272 mg, 3.2 mmol), piperidine (290 mg, 3.4 mmol) and $CHCl_3$ (10 mL). A dark red solid (185 mg) has been isolated as the product with 91 % of yield. ^{1}H NMR (500 MHz, DMSO-d_6) δ 8.03 (s, 2H), 7.75 (dd, *J* = 8.5, 2.0 Hz, 2H), 7.72 (d, *J* = 2.0 Hz, 2H), 7.52 (d, *J* = 3.8 Hz, 2H), 7.31 (d, *J* = 3.7 Hz, 2H), 7.19 (d, *J* = 8.8 Hz, 2H), 3.97 (t, *J* = 6.9 Hz, 2H), 1.70 (quint, *J* = 7.0 Hz, 2H), 1.39 (quint, *J* = 7.0 Hz, 2H), 1.31 – 1.15 (m, 8H), 0.81 (t, *J* = 6.8 Hz, 3H). ^{13}C NMR (126 MHz, DMSO-d_6) δ 164.43, 158.54, 147.78, 145.30, 137.89, 125.28, 123.99, 123.78, 123.67, 117.20, 116.99, 31.54, 29.05, 28.89, 26.52, 26.35, 22.46, 14.35. Anal. Calcd. For : C, 68.23; H, 4.93; N,6.63. Found: C,68.11; H,5.31; N,6.69.

3,3'-(5,5'-(10-octyl-10*H*-phenooxazine-3,7-diyl)bis(thiophene-5,2-diyl))bis(2-cyanoacrylic acid) (POZ-Th). **POZ-Th** was synthetized according to general procedure for Knoevenagel condensation using product **2c** (50 mg, 0.097 mmol), cyanoacetic acid (82 mg, 0.97 mmol), piperidine (103 mg, 1.16 mmol) and $CHCl_3$ (5 mL). A dark red solid (58 mg) has been isolated as the product with quantitative yield. ^{1}H-NMR (DMSO-d_6, 500 MHz): δ 8.35 (s, 2H), 7.87 (d, 2H, *J* = 4.2 Hz), 7.53 (d, 2H, *J* = 4.0 Hz), 7.16 (dd, 2H, *J* = 8.2, 1.8 Hz), 6.93 (d, 2H, *J* = 1.9 Hz), 6.65 (d, 2H, *J* = 8.7 Hz), 3.48 (broad s, 2H), 1.51 (broad s, 2H), 1.40-1.10 (m, 10H), 0.85 (t, 3H, *J* = 6.7 Hz). ^{13}C-NMR (DMSO-d_6, 126 MHz): δ 164.21, 152.76, 146.77, 144.40, 141.81, 133.73, 133.41, 125.92, 124.27, 122.96, 117.04, 113.07, 112.61, 97.56, 31.70, 29.26, 29.22, 26.53, 25.10, 22.56, 14.40. Anal. Calcd. For : C, 66.54; H, 4.81; N, 6.47. Found: C, 66.64; H, 4.64; N 6.17.

3,3'-(5,5'-(10-octyl-10*H*-phenooxazine-3,7-diyl)bis(furanen-5,2-diyl))bis(2-cyanoacrylic acid) (POZ-Fu). **POZ-Fu** was synthetized according to general procedure for Knoevenagel condensation using product **2d** (200 mg, 0.41 mmol), cyanoacetic acid (349 mg, 4.1 mmol), piperidine (431 mg, 4.92 mmol) and $CHCl_3$ (5 mL). A dark red solid (190 mg) has been isolated as the product with 75 % of yield. ^{1}H NMR (500 MHz, DMSO-d_6): δ 7.89 (s, 2H), 7.38 (d, 2H, J = 3.5 Hz), 7.36 (d, 2H, J = 8.9 Hz), 7.16 (d, 2H, J = 3.4 Hz), 7.14 (s, 2H), 6.76 (d, 2H, J = 8.6 Hz), 3.56 (broad s, 2H), 1.54 (broad s, 2H), 1.45-1.15 (m, 10H), 0.85 (t, 3H, J = 6.2 Hz). ^{13}C-NMR (DMSO-d_6, 125 MHz): δ 164.64, 158.27, 147.69, 144.46, 136.73, 133.49, 122.31, 121.99, 117.76, 113.15, 111.62, 109.13, 43.75, 31.69, 29.23, 26.45, 25.11, 22.54, 14.39. Anal. Calcd. For : C, 70.01; H, 5.06; N, 6.80. Found: C, 70.04; H, 5.39; N,6.73.

5,5'-(9-Octyl-9H-carbazole-3,6-diyl)bis(thiophene-5,2-diyl))bis(2-cyanoacrylic acid) (CBZ-Th). **CBZ-Th** was synthetized according to general procedure for Knoevenagel condensation using product **2e** (210 mg, 0.42 mmol), cyanoacetic acid (370 mg, 4.35 mmol), piperidine (384 mg, 4.5 mmol) and $CHCl_3$ (5 mL). A dark red solid (187 mg) has been isolated as the product with 71 % of yield. ^{1}H NMR (500 MHz, DMSO-d_6): δ 8.80 (d, J = 1.8 Hz, 2H), 8.51 (s, 2H), 8.06 (d, J = 4.2 Hz, 2H), 7.93 (dd, J = 8.6 Hz, 1.9 Hz, 2H), 7.84 (d, J = 4.1 Hz, 2H), 7.74 (d, J = 8.7 Hz, 2H), 4.45 (t, J = 6.7 Hz, 2H), 1.80 (q, J = 7.2 Hz, 2H), 1.33-1.12 (m, 10H), 0.80 (t, J = 6.9 Hz, 3H). Anal. Calcd. For : C, 68.22; H, 4.93; N,6.63. Found: C, 68.07; H, 5.09; N, 7.03.

5,5'-(9-Octyl-9H-carbazole-3,6-diyl)bis(furanen-5,2-diyl))bis(2-cyanoacrylic acid) (CBZ-Fu). **CBZ-Fu** was synthetized according to general procedure for Knoevenagel condensation using product **2f** (159 mg, 0.34 mmol), cyanoacetic acid (275 mg, 3.23 mmol), piperidine (300 mg, 3.5 mmol) and $CHCl_3$ (5 mL). A dark red solid (110 mg) has been isolated as the product with 53 % of yield. ^{1}H NMR (500 MHz, DMSO-d_6): δ 8.67 (s, 2H), 8.02 (d, J = 8.5 Hz, 2H), 7.94 (s, 2H), 7.74 (d, J = 8.5 Hz, 2H), 7.40 (d, J = 3.2 Hz, 2H), 7.21 (d, J = 3.2 Hz, 2H), 4.41 (s, 2H), 1.77 (d, J = 6.0 Hz, 2H), 1.31-1.10 (m, 10H), 0.80 (t, J = 7.0 Hz, 3H). ^{13}C NMR (126 MHz, DMSO-d_6) δ 158.60, 148.22, 141.41, 123.68, 122.90, 121.18, 119.08, 117.55, 110.97, 43.12, 31.58, 29.12, 29.02, 28.97, 26.85, 22.43, 14.32. Anal. Calcd. For : C, 71.87; H, 5.19; N, 6.98. Found: C, 71.47; H, 5.48; N,6.60.

Electrochemical characterization

Pulsed Voltammetry (DPV) and Cyclic Voltammetry (CV) were carried out at scan rate of 20 and 50 mV/s, respectively, using a PARSTA2273 potentiostat in a two compartments, three electrode electrochemical cell in a glove box filled with N_2 ([O_2] and [H_2O] ≤ 0.1 ppm). The working, counter, and the pseudo-reference electrodes were a glassy carbon pin, a Pt flag and an Ag/AgCl wire, respectively. The working electrodes discs were well polished with alumina 0.1 μm suspension, sonicated for 15 min in deionized water, washed with 2-propanol, and cycled for 50 times in 0.5 M H_2SO_4 before use. The Ag/AgCl pseudo-reference electrode was calibrated, by adding ferrocene (10^{-3} M) to the test solution after each measurement.

Preparation of Pt/TiO_2 nanopowder

Platinization of TiO2 Degussa P25 was done through a photodeposition method known in literature.[4-7] TiO_2 Degussa P25 (2.0 g) was suspended in a solution of H_2O (200 mL) and EtOH (200 mL) containing 32.7 mg of $Pt(NO_3)_2$, in order to reach a final metal loading of 1.0 wt%. After stirring for 1 h in the dark, the suspension was irradiated with a 450 W medium pressure lamp for 4 h. Nanopowders were recovered through centrifugation, washed with EtOH 3 times, and dried under vacuum at 50 °C overnight.

Characterization of Pt/TiO_2 nanopowder

Phase composition has been analysed by Powder X-ray Diffraction (PXRD) using a Philips X'Pert diffractometer using a Cu Kα (λ = 0.154 nm) X-ray source in the range 10° < 2θ < 100° and data were analyzed by using the PowderCell 2.0 software. Mean crystallite sizes were calculated applying the Scherrer's equation to the principal reflection of each phase [(101) for anatase and (110) for rutile].

Textural properties of the catalyst has been analyzed by N_2 physisorption at the liquid nitrogen temperature using a Micromeritics ASAP 2020 automatic analyzer. The samples were previously degassed under vacuum at 200°C overnight. Specific surface area has been determined applying the BET method to the adsorption isotherm in the range $0.10 < p/p^0 < 0.35$. Pore size distribution has been evaluated applying the BJH theory to the desorption branch of the isotherm.[8]

The morphology of the composite materials and the distribution of the supported Pt nanoparticles were evaluated by High Resolution Transmission Electron Microscopy (HR-TEM) and High Angle Annular Dark Field-Scanning Transmission Electron Microscopy (HAADF-STEM) images recorded by a JEOL 2010-FEG microscope operating at the acceleration voltage of 200 kV. The microscope has 0.19 nm spatial resolution at Scherzer defocus conditions in HR-TEM mode and a probe of 0.5 nm was used in HAADF-STEM mode.

Adsorption of PTZs, POZs, CBZs dyes on Pt/TiO_2

Dye staining was done by suspending 200 mg of Pt/TiO_2 nanopowders in 20 mL of dye solution (0.3 mM in ethanol) for 24 h in the dark. Then nanopowders were separated through centrifugation, washed twice with ethanol, and dried under vacuum at room temperature overnight. After adsorption, the concentration of the dyes in the solution was measured by UV-vis spectroscopy, confirming that the loading of dyes on the Pt/TiO_2 material is quantitative.

Hydrogen production through water splitting

The dye-functionalized Pt/TiO_2 nanomaterials have been tested for H_2 production following a procedure previously described.[1] 50 mg of the dye-functionalized Pt/TiO_2 catalyst was suspended into 60 mL of 10 % v/v aqueous solution of triethanolamine (TEOA) previously neutralized with HCl. After purging with Ar (15 mL min^{-1}) for 30 min, the suspension was irradiated using a 150 W Xe lamp with a cut-off filter at 420 nm. Irradiance was ~ 6 x 10^{-3} W m^{-2} in the UV-A range and ~ 1080 W m^{-2} in the visible range (400 – 1000 nm). The concentration of H_2 in gas stream coming from the reactor has been quantified using a Agilent 7890 gaschromatograph equipped with a TCD detector, connected to a Carboxen 1010 column (Supelco, 30 m x 0.53 mm ID, 30 μm film) using Ar as carrier.

The performances of the sensitized photocatalysts have been reported in terms of H_2 production rate and overall H_2 productivity. Turn-Over Numbers (TON) were calculated as:

$$\mathrm{TON} = \frac{2 \text{ x overall } H_2 \text{ amount } (\mu\mathrm{mol\ g^{-1}})}{\text{dye loading } (\mu\mathrm{mol\ g^{-1}})}$$

Light-to-Fuel Efficiency (LFE) was calculated as:

$$\mathrm{LFE} = \frac{F_{H_2} \times \Delta H^0_{H_2}}{S \times A_{irr}}$$

where F_{H2} is the flow of H_2 produced (expressed in mol s^{-1}), ΔH^0_{H2} is the enthalpy associated with H_2 combustion (285.8 kJ mol^{-1}), S is the total incident light irradiance, as measured by adequate radiometers in 400 – 1000 nm ranges (expressed in W cm^{-2}) and A_{irr} is the irradiated area (expressed in cm^2). UV-vis spectra of the aqueous solutions recovered at the end of the photocatalytic runs highlighted that no desorption of the dyes took place during the experiments.

1. Cecconi, B.; Manfredi, N.; Ruffo, R.; Montini, T.; Romero-Ocana, I.; Fornasiero, P.; Abbotto, A. *ChemSusChem* **2015,** *8*, 4216-28.
2. Grisorio, R.; De Marco, L.; Allegretta, G.; Giannuzzi, R.; Suranna, G. P.; Manca, M.; Mastrorilli, P.; Gigli, G. *Dyes Pigm.* **2013,** *98*, 221-231.
3. Soloducho, J.; Doskocz, J.; Nowakowska, A.; Cabaj, J.; Lapkowski, M.; Golba, S. *Pol. J. Chem.* **2007,** *81*, 2001 - 2012.
4. Bae, E.; Choi, W.; Park, J.; Shin, H. S.; Kim, S. B.; Lee, J. S. *J. Phys. Chem. B* **2004,** *108*, 14093-14101.
5. Lee, S. H.; Park, Y.; Wee, K. R.; Son, H. J.; Cho, D. W.; Pac, C.; Choi, W.; Kang, S. O. *Org Lett* **2010,** *12*, 460-3.
6. Montini, T.; Gombac, V.; Sordelli, L.; Delgado, J. J.; Chen, X.; Adami, G.; Fornasiero, P. *ChemCatChem* **2011,** *3*, 574-577.
7. Romero Ocaña, I.; Beltram, A.; Delgado Jaén, J. J.; Adami, G.; Montini, T.; Fornasiero, P. *Inorg. Chim. Acta* **2015,** *431*, 197-205.
8. Sing, K. S. W.; Everett, D. H.; Haul, R. A. W.; Moscou, L.; Pierotti, R. A.; Rouquerol, J.; Siemieniewska, T. *Pure Appl. Chem.* **1985**, *57*, 603.

Table S1. Main optical and electrochemical characterization of the **PTZs**, **CBZs** and **POZs** dyes.

Sample	λ_{max} [a] (nm)	ε ($M^{-1}cm^{-1}$)	V_{ox} (V vs. Fc) ± 10 mV	HOMO[b] (eV) ± 0.05 eV	E_{gap}^{opt} (eV)	LUMO[b] eV ± 0.05 eV
PTZ-Th[c]	470	34000 ± 1000	0.15	-5.38	2.05	-3.33
PTZ-Fu	481	30200 ± 700	0.36	-5.59	1.98	-3.61
POZ-Th	534	31800 ± 1500	0.41	-5.64	1.87	-3.77
POZ-Fu	524	27200 ± 200	0.38	-5.61	1.90	-3.71
CBZ-Th	414	35800 ± 100	0.41	-5.64	2.26	-3.38
CBZ-Fu	409	41800 ± 600	0.43	-5.66	2.28	-3.38

[a] Dye solution 10^{-5} M in THF. [b] Vacuum potential = Fc/Fc^{+} + 5.23 V. [c] Values from Ref 1; CV and DPV plots are reported in Ref 1.

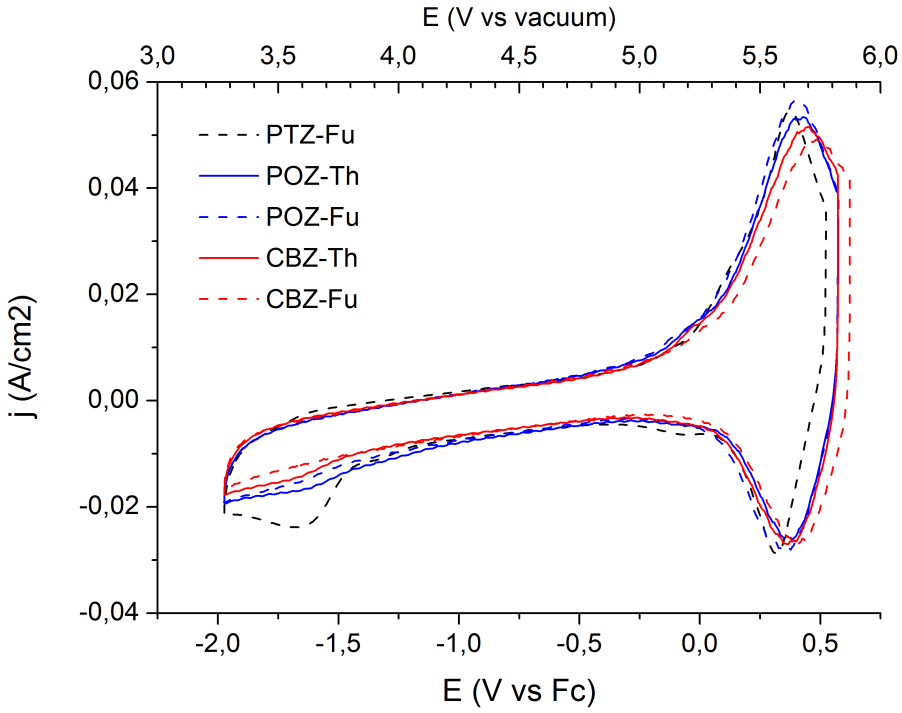

Figure S1. Ciclic voltammetry (CV) of the **PTZs**, **CBZs** and **POZs** dyes recorded in ACN:CH_2Cl_2 3:1 $TBAClO_4$ 0.075M solution.

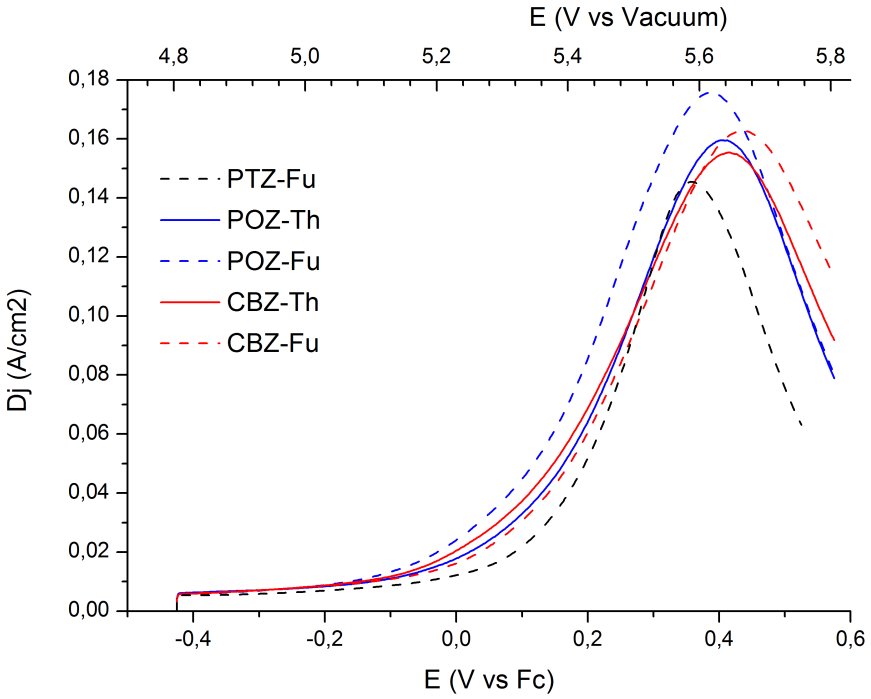

Figure S2. Differential pulse voltammetry (DPV) of the **PTZs**, **CBZs** and **POZs** dyes recorded in ACN:CH_2Cl_2 3:1 $TBAClO_4$ 0.075M solution.

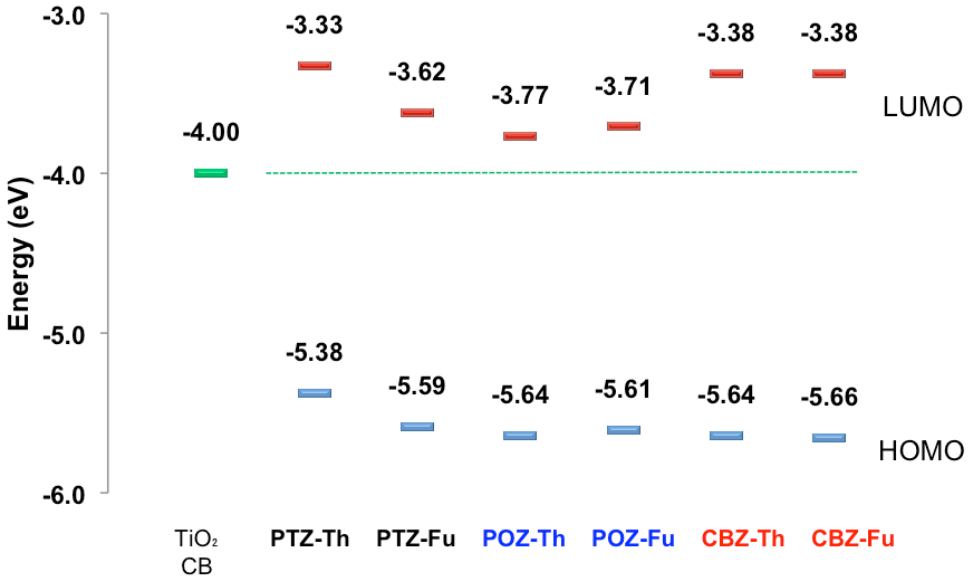

Figure S3. Experimental HOMO/LUMO energy levels for the dyes investigated in this work (CB level of TiO_2 is included as a reference for electron injection from the dye to the semiconductor).

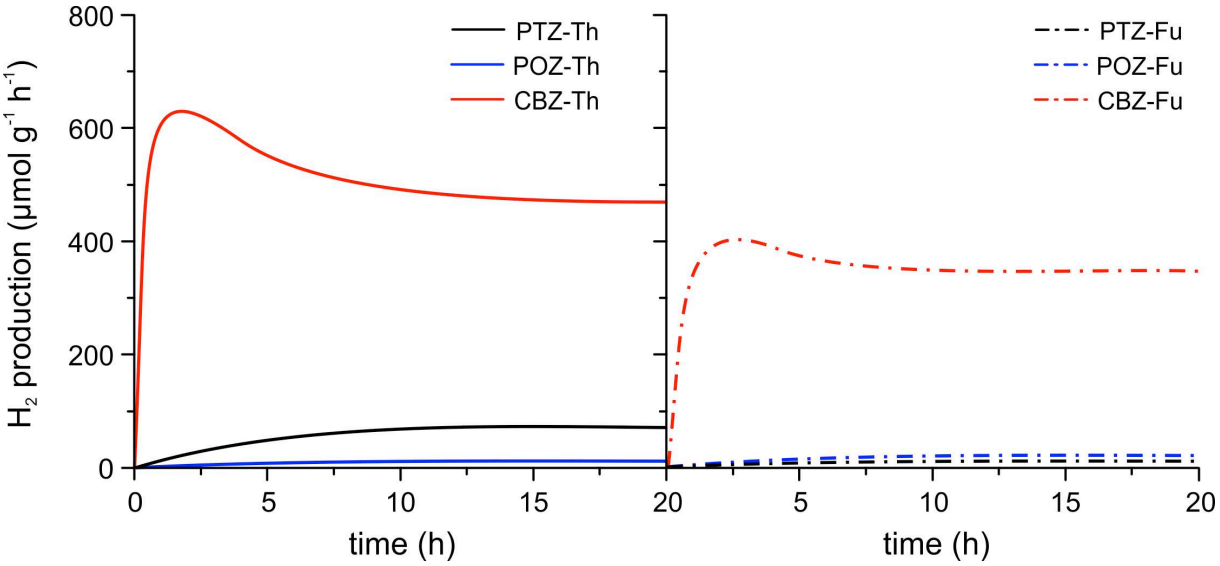

Figure S4. H_2 production from TEOA 10% v/v solution at pH = 7.0 under irradiation with visible light (λ > 420 nm) over Pt/TiO_2 materials sensitized with **PTZs**, **POZs** and **CBZs** dyes.

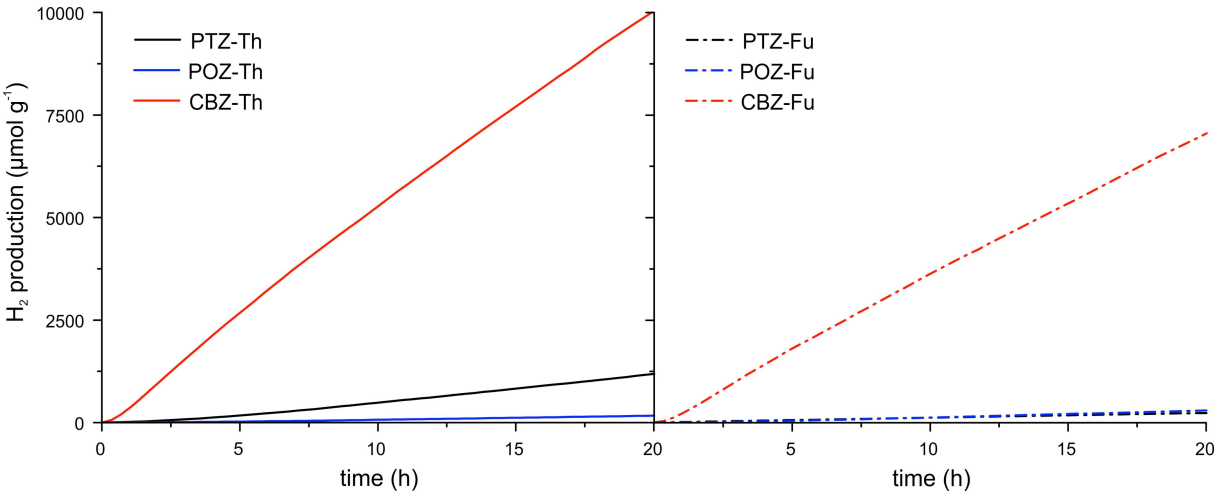

Figure S5. H_2 production from TEOA 10% v/v solution at pH = 7.0 under irradiation with visible light (λ > 420 nm) over Pt/TiO_2 materials sensitized with **PTZs**, **POZs** and **CBZs** dyes.

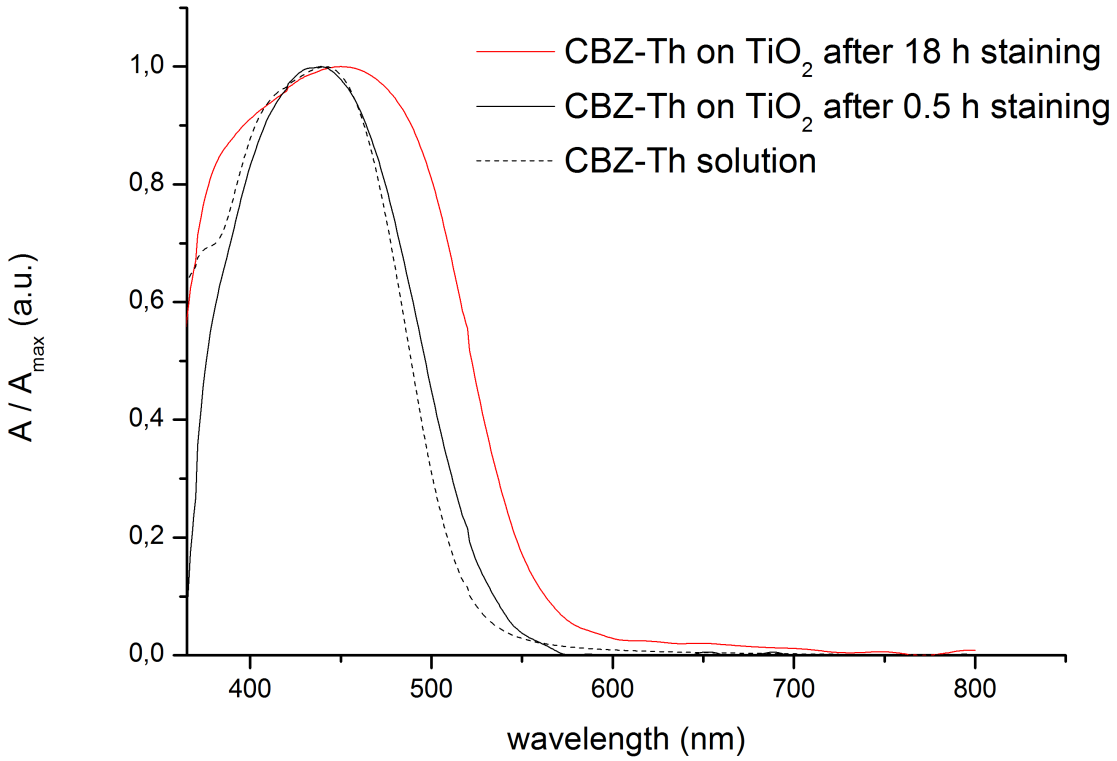

Figure S6. Normalized absorption spectra of **CBZ-Th** on 3 µm transparent TiO_2 films at different staining times and comparison with absorption spectra as a DMSO solution.

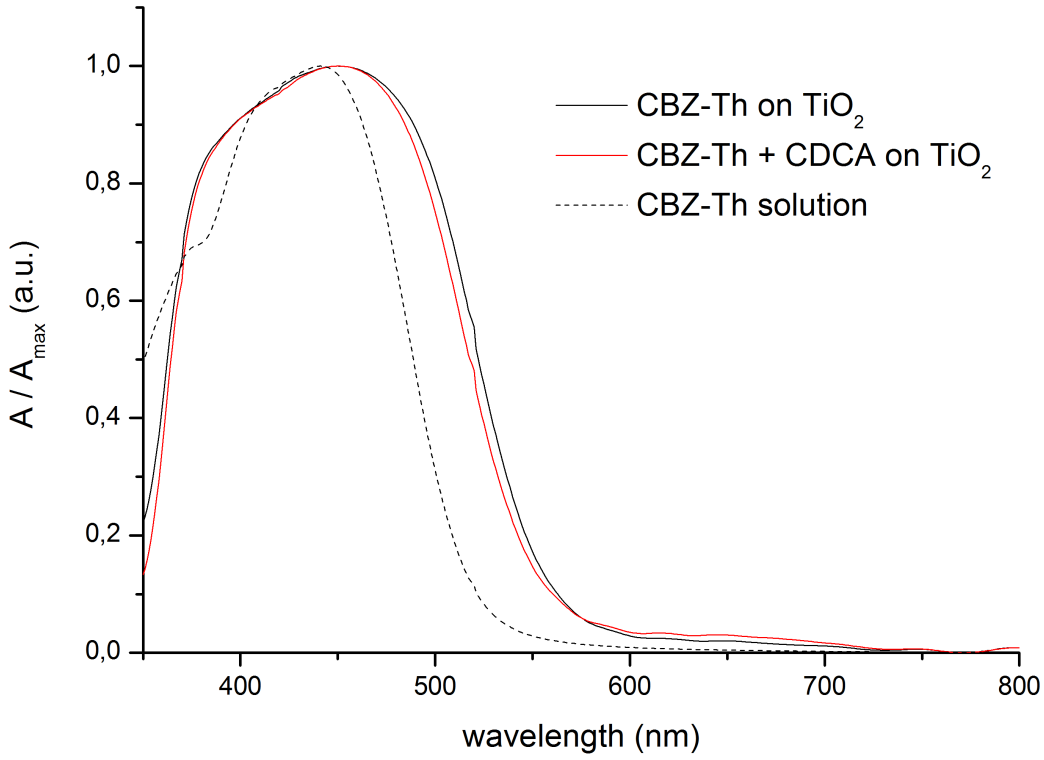

Figure S7. Normalized absorption spectra of **CBZ-Th** on 3 µm transparent TiO_2 films (black line), in presence of 100:1 CDCA (red line), and comparison with absorption spectra as a DMSO solution. (black dashed line).

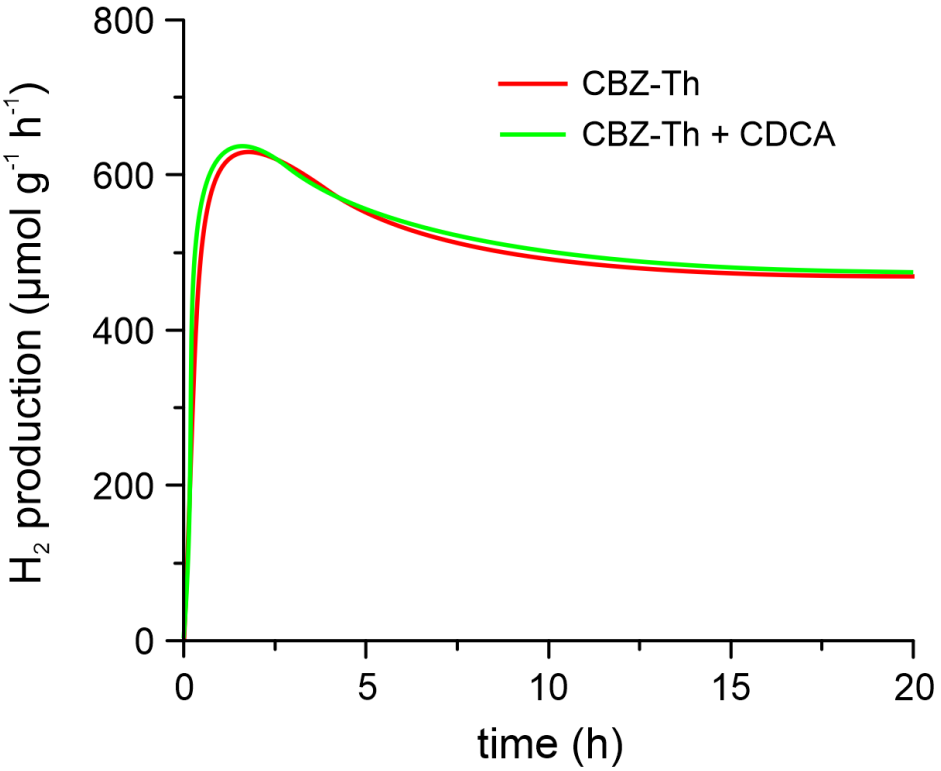

Figure S8 H_2 production from TEOA 10% v/v solution at pH = 7.0 under irradiation with visible light (λ > 420 nm) over Pt/TiO_2 materials sensitized with the CBZ-Th dye (red) and with CBZ-Th+CDCA 1:1 mol (green)

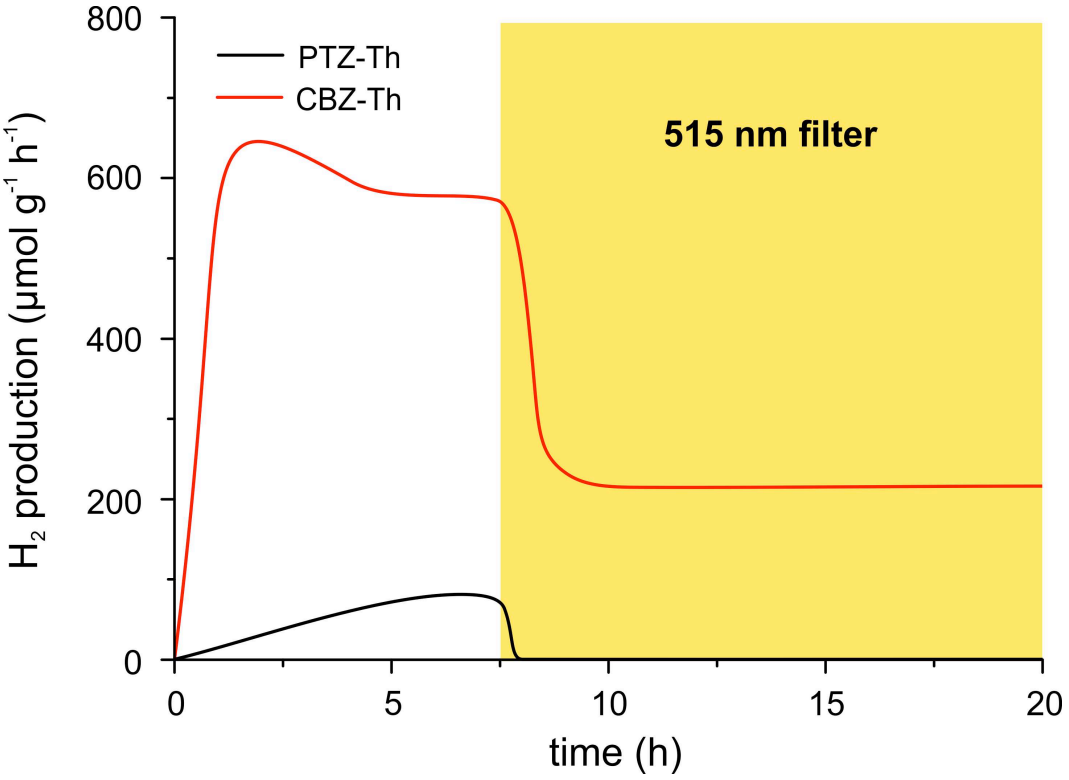

Figure S9. H_2 production from TEOA 10% v/v solution at pH = 7.0 over Pt/TiO_2 materials sensitized with **PTZ-Th** and **CBZ-Th** dyes: after activation under irradiation with visible light (λ > 420 nm) for 8h, the photocatalytic activity under irradiation with photons with λ > 515 nm is presented.

Table S2. TON values and LFE_{20} for **PTZs**, **POZs**, and **CBZs** sensitized catalysts.

Dye sensitizer	H_2 amount ($\mu mol\ g^{-1}$ at 20h)	TON ($\mu mol(H_2)\ \mu mol(dye)^{-1}$ at 20h)	LFE_{20} (%)
PTZ-Th	1178	236	0.032%
PTZ-Fu	227	45	0.006%
POZ-Th	163	33	0.004%
POZ-Fu	294	59	0.008%
CBZ-Th	10083	2017	0.272%
CBZ-Fu	7064	1413	0.190%

^{1}H-NMR and ^{13}C-NMR spectra

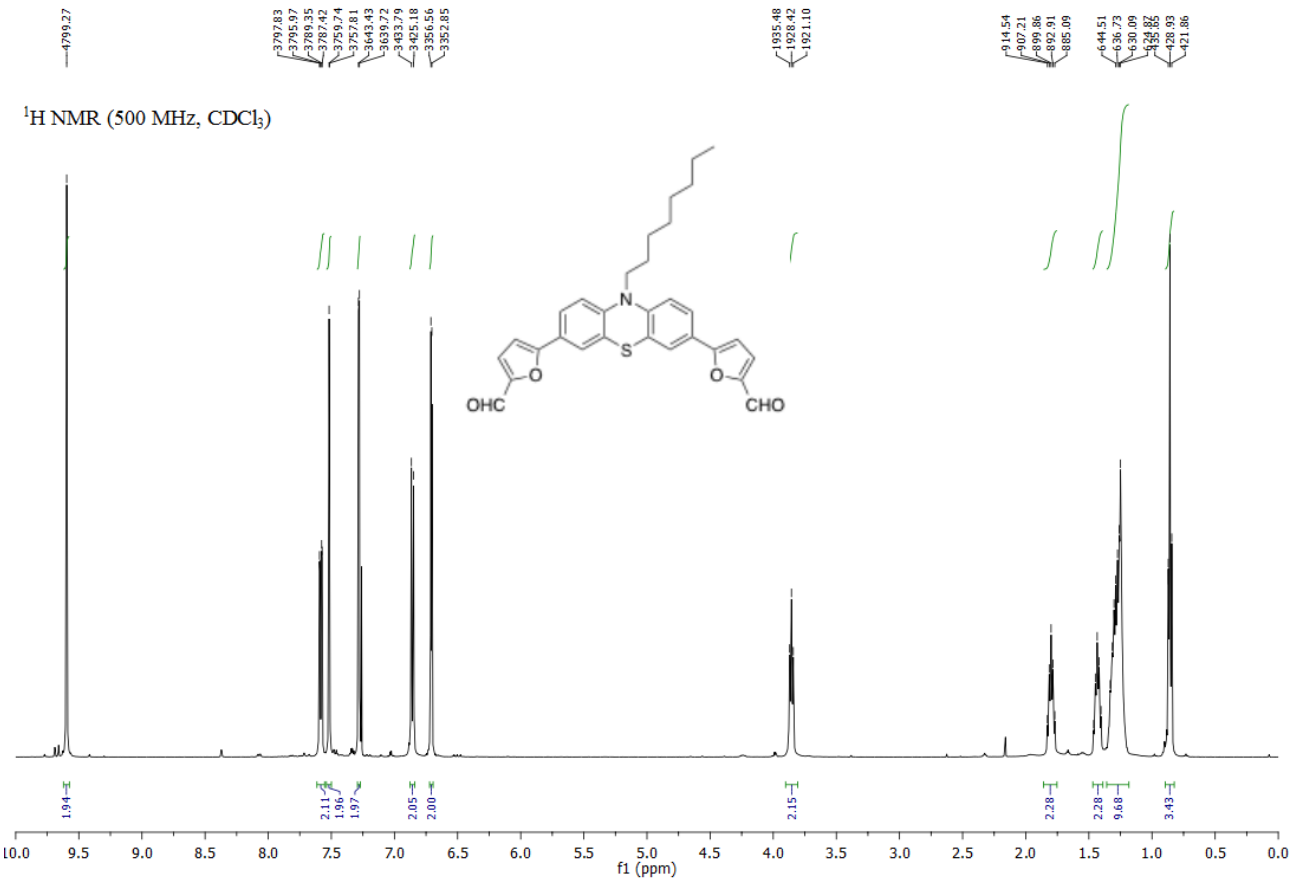

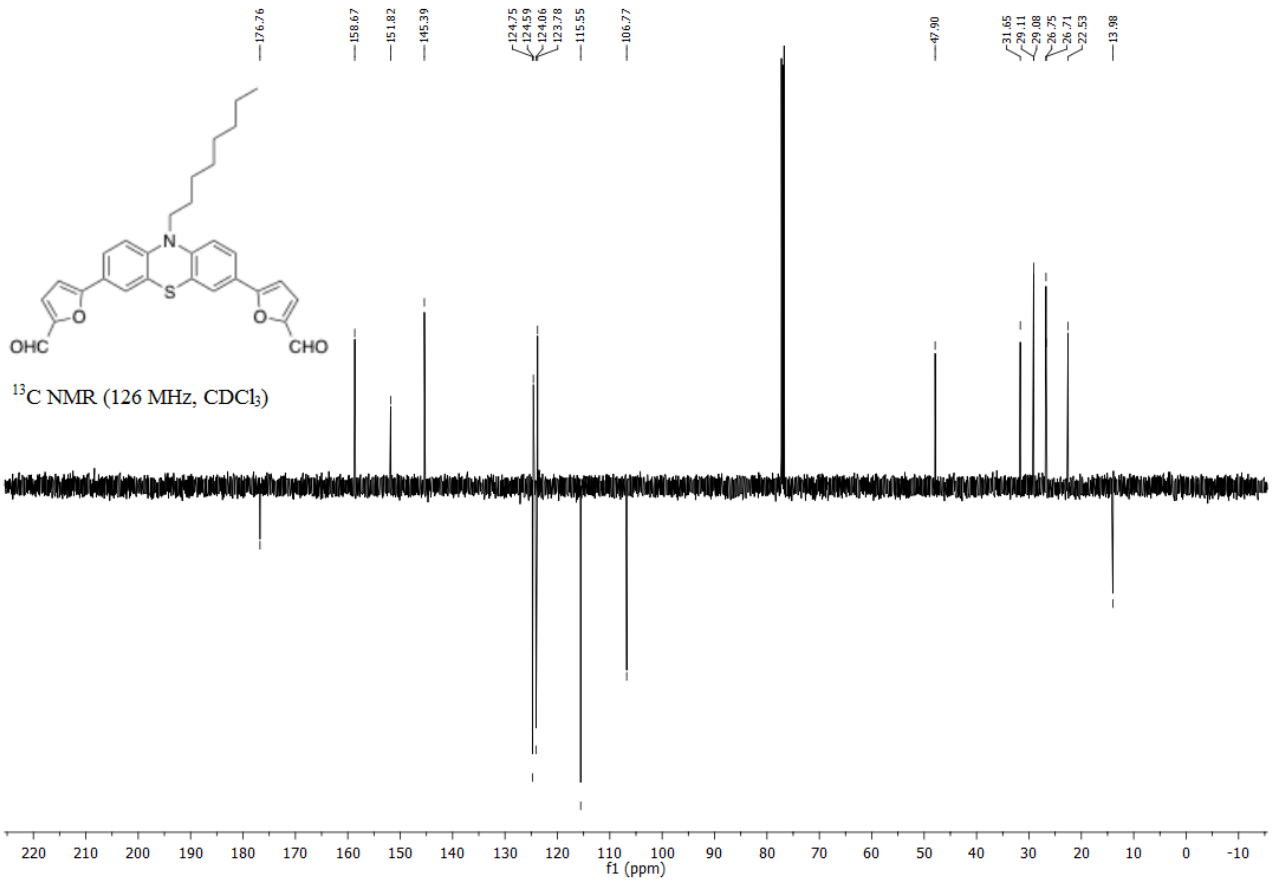

^{13}C NMR (126 MHz, $CDCl_3$)

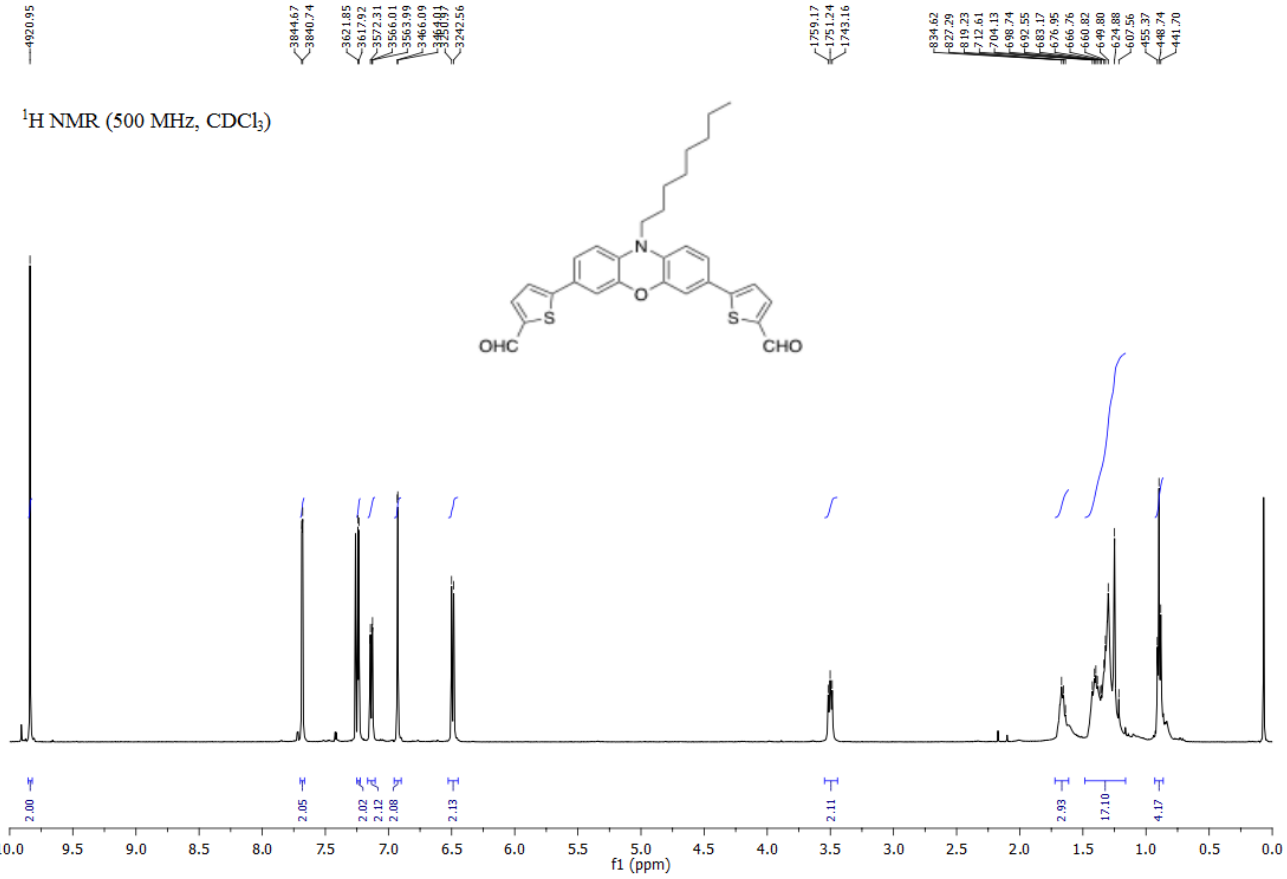

^{1}H NMR (500 MHz, $CDCl_3$)

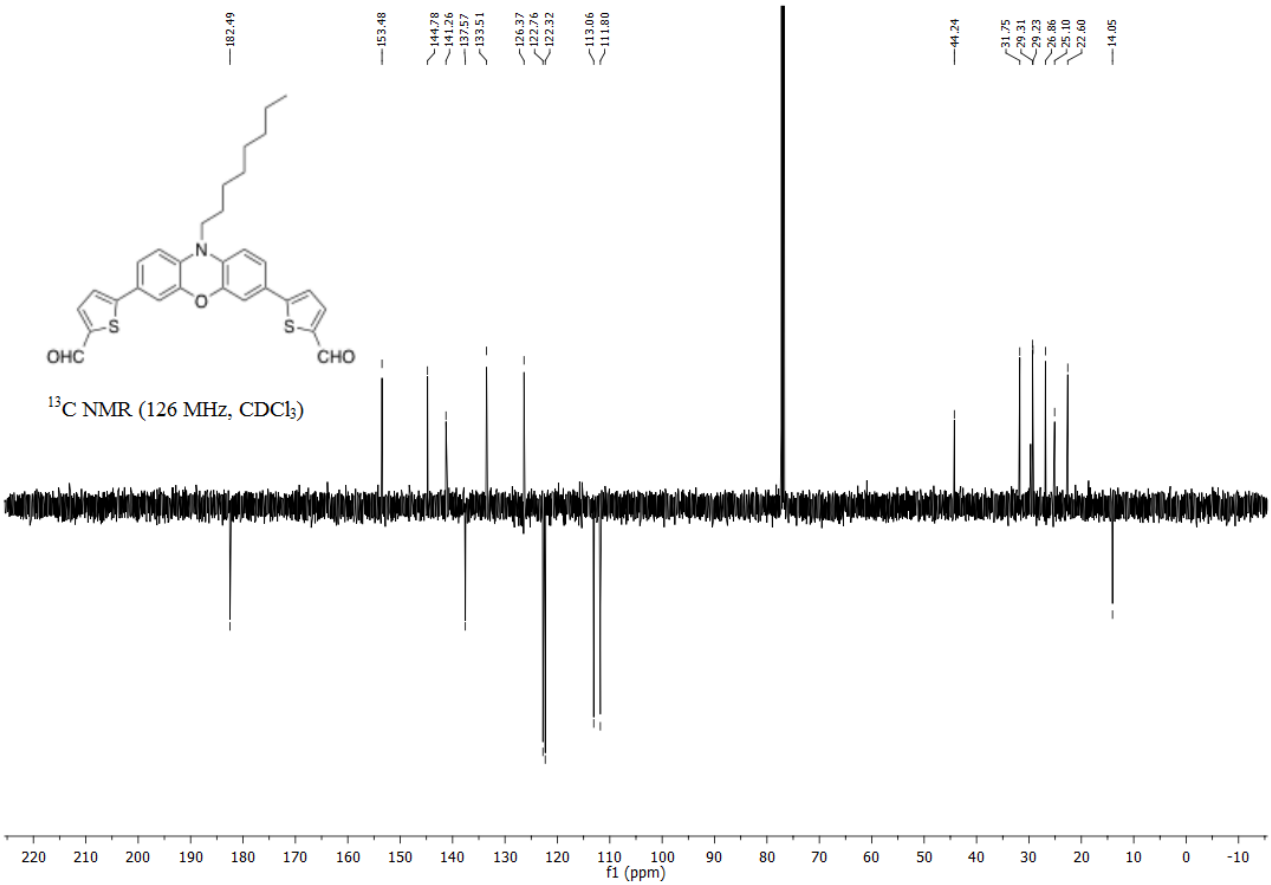
182.49
153.48
144.78
141.26
137.57
133.51
126.37
122.76
122.32
113.06
111.80
44.24
31.75
29.31
29.23
26.86
25.10
22.60
14.05
OHC
CHO
S
S
N
O
13C NMR (126 MHz, CDCl3)
f1 (ppm)

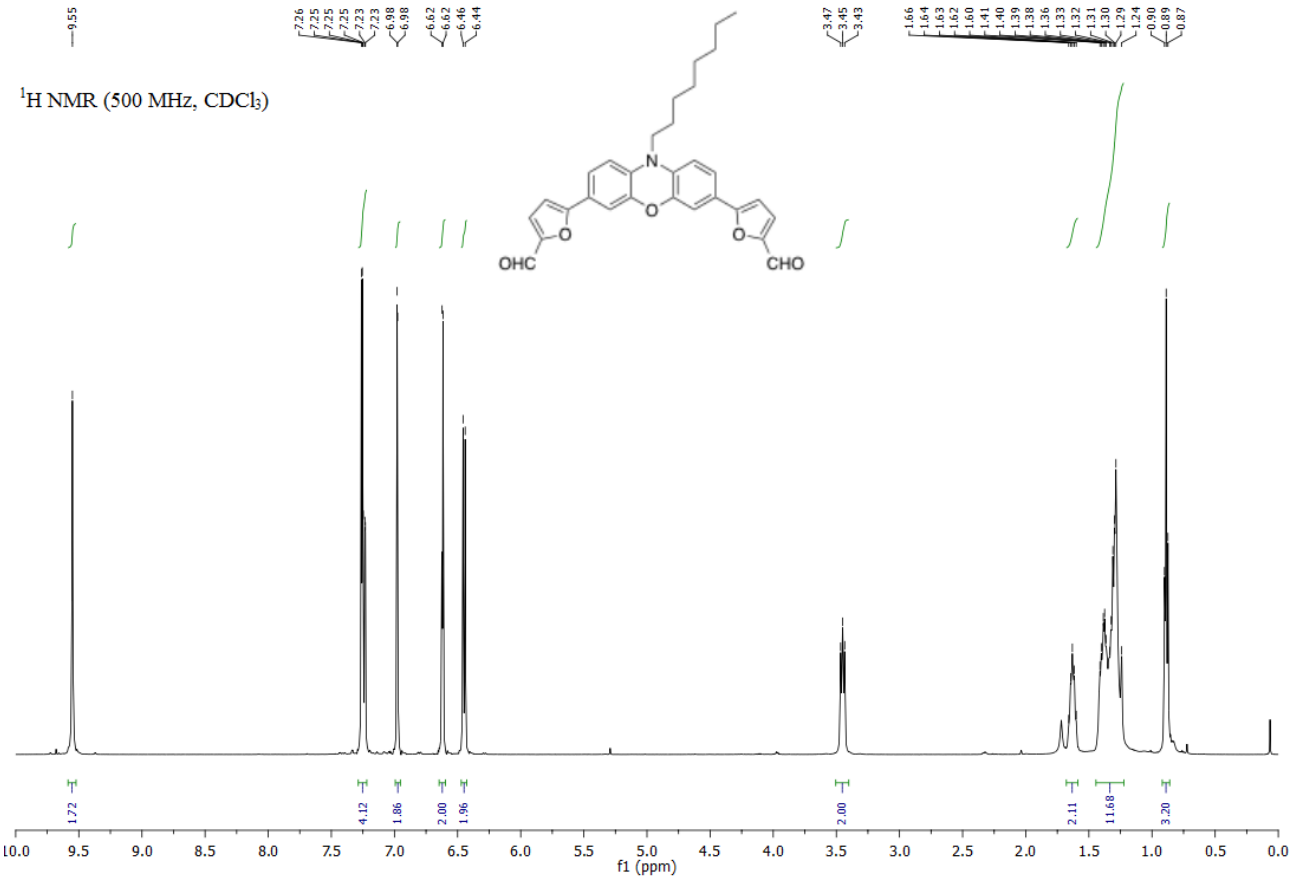
9.55
7.26
7.25
7.25
7.25
7.23
7.23
6.98
6.98
6.62
6.62
6.46
6.44
3.47
3.45
3.43
1.66
1.64
1.63
1.62
1.60
1.41
1.40
1.39
1.38
1.36
1.33
1.32
1.31
1.30
1.29
1.24
0.90
0.89
0.87
1H NMR (500 MHz, CDCl3)
OHC
CHO
O
O
N
O
1.72
4.12
1.86
2.00
1.96
2.00
2.11
11.68
3.20
f1 (ppm)

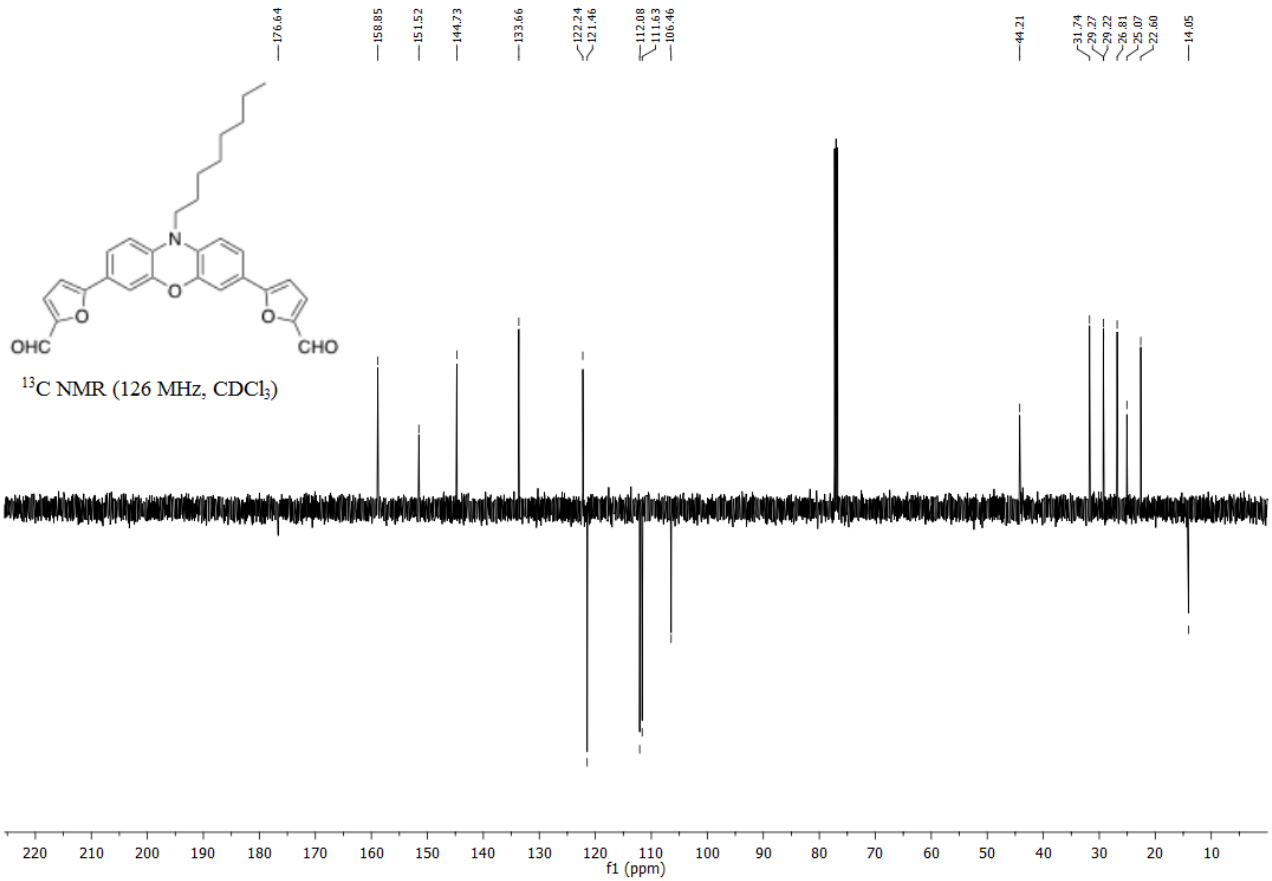
176.64
158.85
151.52
144.73
133.66
122.24
121.46
112.08
111.63
106.46
44.21
31.74
29.27
29.22
26.81
25.07
22.60
14.05
OHC
CHO
13C NMR (126 MHz, CDCl3)
f1 (ppm)

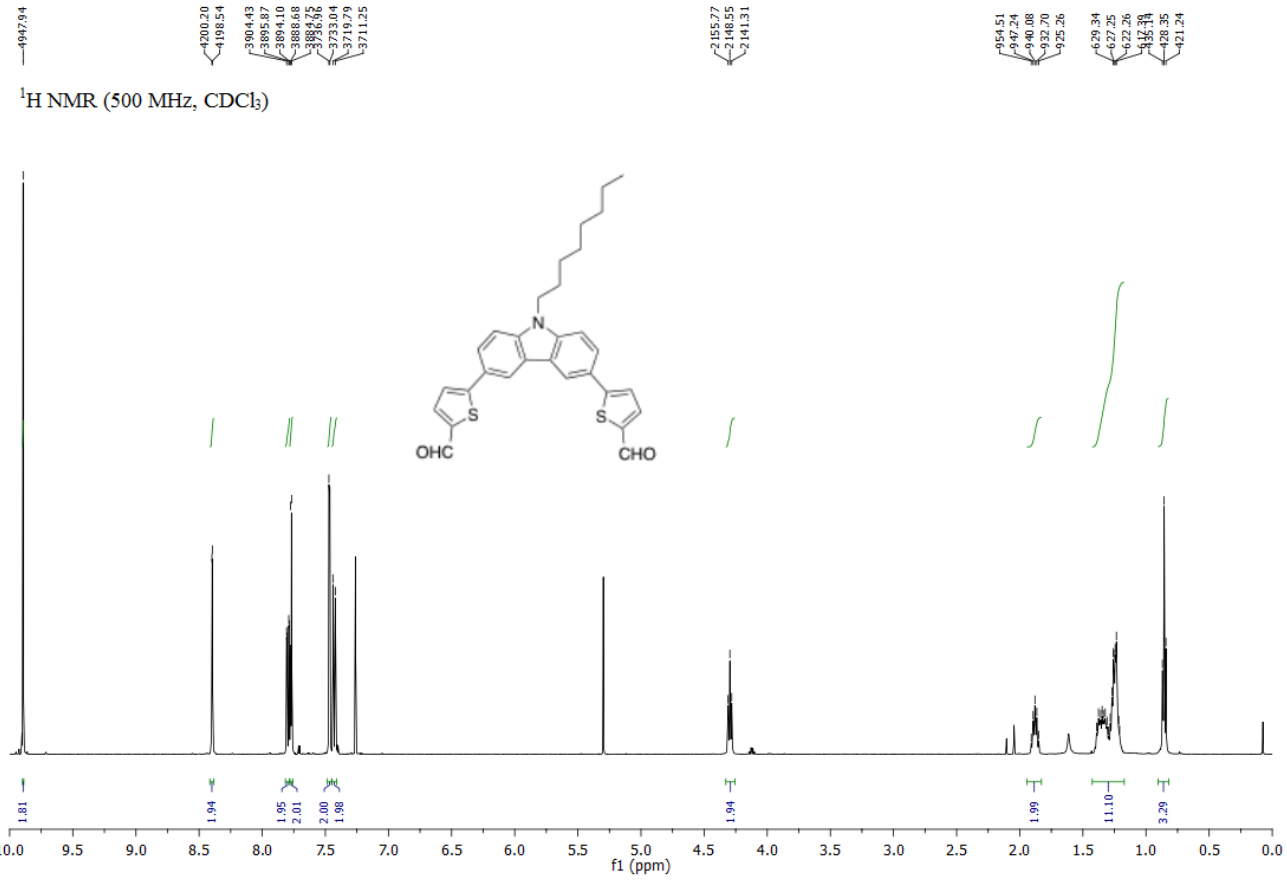
7.94
4200.20
4198.54
3904.43
3895.87
3894.10
3888.68
3733.04
3719.79
3711.25
2155.77
2148.55
2141.31
954.51
947.24
940.08
932.70
925.26
629.34
627.25
622.26
428.35
421.24
OHC
CHO
1H NMR (500 MHz, CDCl3)
1.81
1.94
1.95
2.01
2.00
1.98
1.94
1.99
11.10
3.29
f1 (ppm)

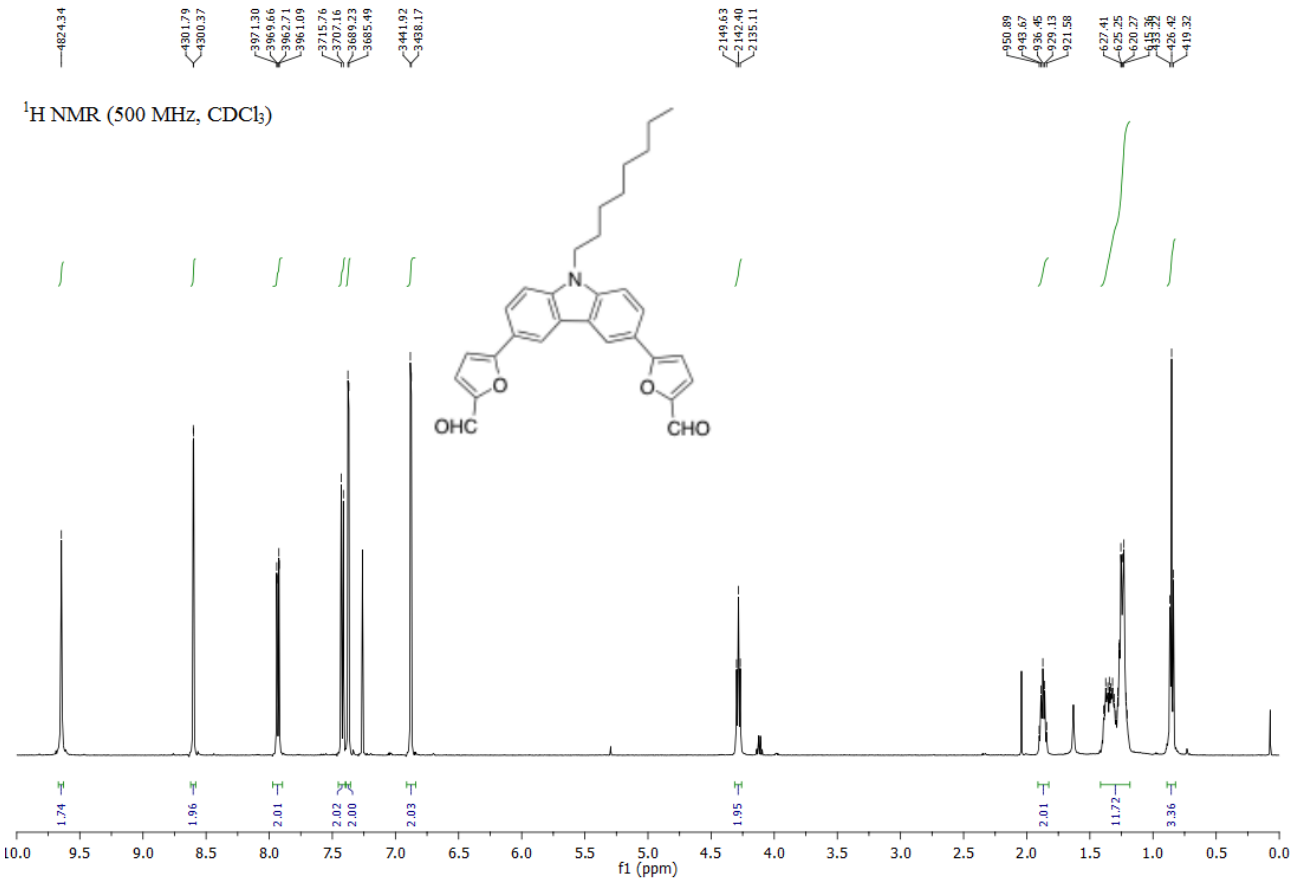
^{1}H NMR (500 MHz, $CDCl_3$)
OHC
CHO
f1 (ppm)

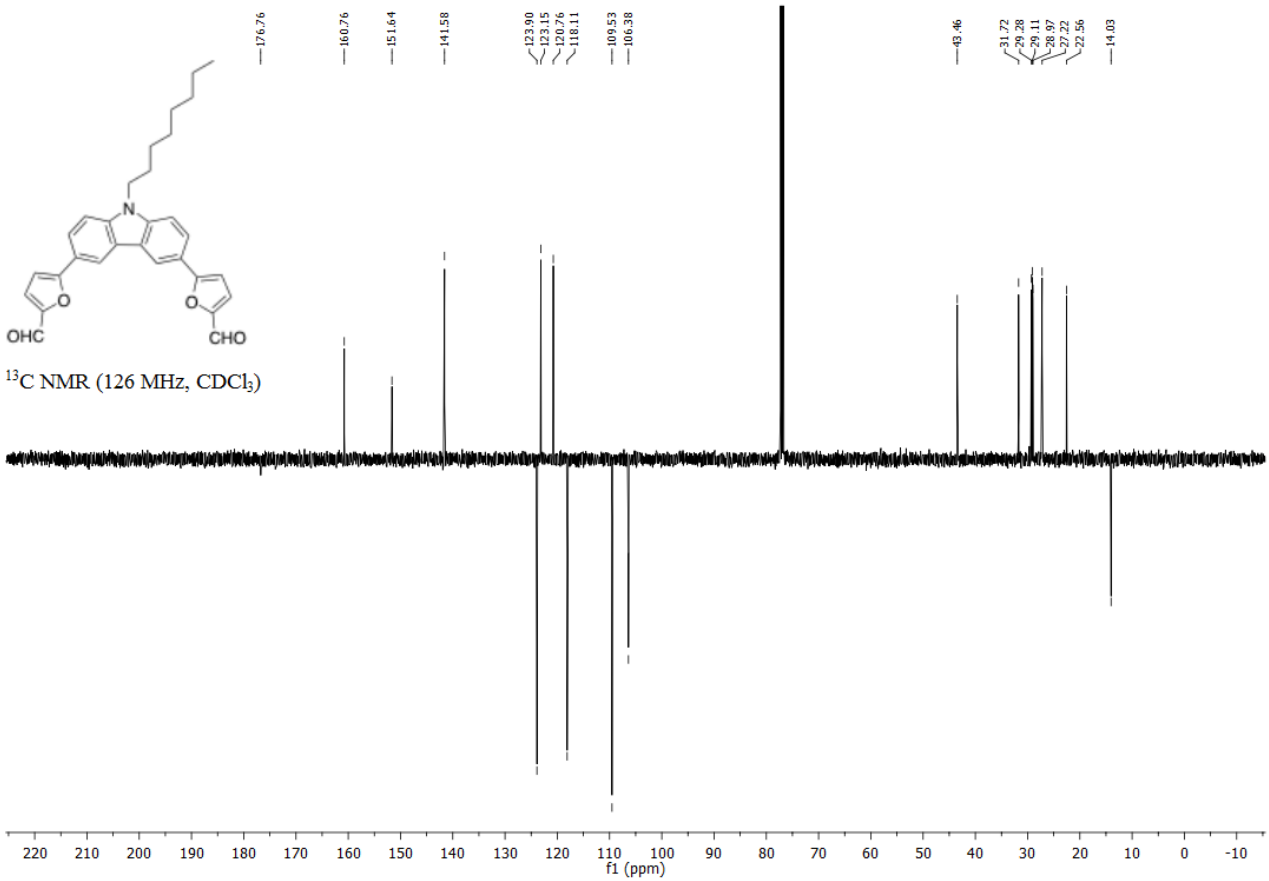
^{13}C NMR (126 MHz, $CDCl_3$)
OHC
CHO
f1 (ppm)

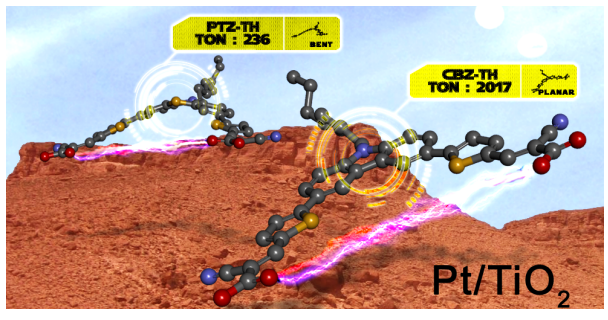

Enhanced photocatalytic hydrogen generation using carbazole-based sensitizers

Norberto Manfredi,*[a] Matteo Monai,[b] Tiziano Montini,[b] Matteo Salamone,[a] Riccardo Ruffo,[a] Paolo Fornasiero,*[,b] Alessando Abbotto*[,a]

Sulphur-free carbazole derivatives have been synthesized and used as photosensitizers in photocatalytic hydrogen generation yielding greatly enhanced H_2 production

University of Milano-Bicocca

Via R. Cozzi 53, I-20125 Milano, Italy
http://www.mater.unimib.it

Milano, 03 February 2017

Prof. Vincent Artero
Editor
Sustainable Energy & Fuels

Dear Professor Artero,

Please find herewith enclosed the manuscript:

"Enhanced photocatalytic hydrogen generation using carbazole-based sensitizers"
by
Norberto Manfredi, Matteo Monai, Tiziano Montini, Matteo Salamone, Riccardo Ruffo, Paolo Fornasiero, and Alessandro Abbotto

that we would like to submit to *Sustainable Energy & Fuels* for publication as a Communication.

After the recent introduction of metal-free donor(D)-π-acceptor(A) organic molecules as relatively stable photosensitizers for water splitting and photocatalytic H_2 production (see for example: Li, F.; Fan, K.; Xu, B.; Gabrielsson, E.; Daniel, Q.; Li, L.; Sun, L. *J. Am. Chem. Soc.*, **2015**, *137*, 9153-9159; Cecconi, B.; Manfredi, N.; Ruffo, R.; Montini, T.; Romero-Ocaña, I.; Fornasiero, P.; Abbotto, A. *ChemSusChem*, **2015**, *8*, 4216-4228, Manfredi, N.; Cecconi, B.; Calabrese, V.; Minotti, A.; Peri, F.; Ruffo, R.; Monai, M.; Romero-Ocana, I.; Montini, T.; Fornasiero, P.; Abbotto, A. *Chem. Commun.* **2016,** *52*, 6977-6980; Cecconi, B.; Manfredi, N.; Montini, T.; Fornasiero, P.; Abbotto, A. *Eur. J. Org. Chem.* **2016,** *2016*, 5194-5215) it appeared that the efficiency of these systems was greatly limited by the peculiar geometric arrangement of the D core (phenothiazine) and to the presence of sulphur atoms both in the D and spacer (thiophene) units.
With the aim of enhancing overall efficiency, we have here designed new sensitizers with focus on the geometry of the D core (replacement of butterfly phenothiazine with planar carbazole) and substitution of sulphur atoms (in addition to the introduction of carbazole we have replaced thiophene with the analogous five-membered ring furan). Indeed, the presence of heteroatoms in the core and spacer moieties of the investigated sensitizers dramatically affected the photocatalytic hydrogen generation in the visible range over Pt/TiO_2. In particular, the sensitizer where both strategies were combined in the same scaffold (sulphur-free planar donor core, CBZ, and sulphur-free five-membered heterocyclic spacers, Fu) afforded top ranked efficiencies compared to state-of-the-art dye-sensitized hydrogen generation and much greater performances compared to other dyes investigated as a comparison. Therefore, a rational design of the sensitizers was shown to be the key to obtain greatly enhanced performances in H_2 photogeneration under visible light irradiation.

Recently, the *Journal* has devoted much attention to new materials for sunlight-driven hydrogen generation

and water splitting (see for instance: Pavliuk, M. V.; Cieslak, A. M.; Abdellah, M.; Budinska, A.; Pullen, S.; Sokolowski, K.; Fernandes, D. L. A.; Szlachetko, J.; Bastos, E. L.; Ott, S.; Hammarstrom, L.; Edvinsson, T.; Lewinski, J.; Sa, J. *Sustainable Energy & Fuels* **2017;** Ngaw, C. K.; Zhao, C.-e.; Wang, V. B.; Kjelleberg, S.; Yang Tan, T. T.; Zhang, Q.; Joachim Loo, S. C. *Sustainable Energy & Fuels* **2017**; Tian, L.; Murowchick, J.; Chen, X. *Sustainable Energy & Fuels* **2017**; May, M. M.; Lackner, D.; Ohlmann, J.; Dimroth, F.; van de Krol, R.; Hannappel, T.; Schwarzburg, K. *Sustainable Energy & Fuels* **2017**.). In particular, many reports on dye-sensitized hydrogen generation in RSC Journals have been related to the design of new and efficient dyes for improved efficiency. Therefore, the search for new efficient dyes represents a strategic aspect of the present research work in the field of artificial photosynthesis. We thus trust that our results can be of interest to the many readers of *the Journal* involved with this topic and, in particular, fully meet the criteria of urgency and significance for a Communication.

Best regards,

Alessandro Abbotto, Paolo Fornasiero and Norberto Manfredi